JOC The Journal of Organic Chemistry

Article

pubs.acs.org/joc

Library of Azabenz-Annulated Core-Extended Perylene Derivatives with Diverse Substitution Patterns and Tunable Electronic and Optical Properties

Marcus Schulze, Michael Philipp, Waldemar Waigel, David Schmidt, and Frank Würthner*

Institut für Organische Chemie and Center for Nanosystems Chemistry, Universität Würzburg, Am Hubland, 97074 Würzburg, Germany

Supporting Information

ABSTRACT: Here, we present a collection of different azabenz-annulated perylene derivatives. By developing new synthetic strategies and improving existing protocols, we have expanded the structural diversity of these dye molecules to a multifunctional class of ligating chromophores. The Pictet–Spengler (PS) reaction of 1-aminoperylenes with different aldehydes is used to modify the terminal substitution pattern. PS transformations of 1,6- and/or 1,7-diamino perylenes result in 2-fold annulated nitrogen-containing coronene-type molecules like *anti*-$(ab)_2$-PBI **15**, *syn*-$(ab)_2$-PBI **16**, and *syn*-$(ab)_2$-PTE **18**. In addition, azabenz-annulated perylene bisanhydrides (ab-PBA **6** and *syn*-$(ab)_2$-PBA **19**) were explored as universal starting materials providing access to any desired imide functionality. Furthermore, a newly developed regioselective nitration procedure for perylene monoimide diesters (PMIDE) enables the synthesis of 1-nitro-PMIDE **10** and thus of azabenz-annulated perylene derivatives with unsymmetric *peri*-substitution patterns (ab-PMIDE **12** and ab-PMIMA **13**). According to our spectroscopic and theoretical investigations, the optical and electrochemical properties of these multifunctional chromophores can easily be modified and adjusted to many desirable applications following the synthetic strategies presented in this work.

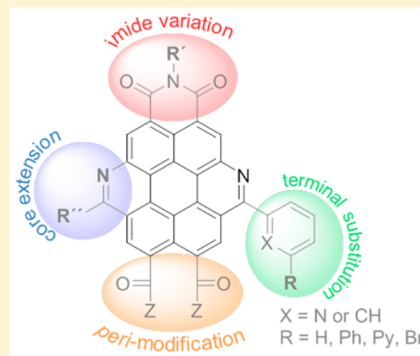

INTRODUCTION

Perylene, one of the most prominent polycyclic aromatic hydrocarbons, constitutes a unique structural motive for many organic dye chemists for more than a century.[1−3] As a consequence of its flat and π-conjugated polyaromatic core, perylene derivatives, in particular the imides and bisimides, were found to be highly desirable (photo)chemically robust colorants with optical absorptions that can be tuned from the near-ultraviolet to the near-infrared spectral region.[4] These diverse optical and electronic properties can be attributed to the exceptional chemistry of perylene with three sets of different carbon atoms located at its edges (Figure 1), four *peri*-(3,4,9,10), four *ortho*- (2,5,8,11), and four *bay*-positions (1,6,7,12), which can be functionalized selectively.

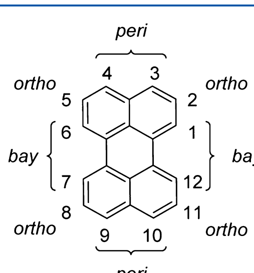

Figure 1. Structure and specific positions of perylene.

Because of the longitudinally oriented transition dipole moment of the lowest energetic optical transition (S_0–S_1), the *peri*-positions have the strongest impact on the photophysical properties of the respective chromophores.[5,6] Particularly, the ester, anhydride, and imide functionalized derivatives of 3,4,9,10-perylene tetracarboxylic acid (abbreviated as PTE (perylene tetraester)), PBA (perylene bisanhydride), and PBI (perylene bisimide)), are of fundamental interest for industry and academia, for example, as industrial organic pigments for the coloration of textiles and automotives, as fluorophore materials for biological sensing, organic electronics (e.g., organic field effect transistors, OFET), and photovoltaics (e.g., bulk heterojunction solar cells, BHJ).[4,7,8] Among the perylene derivatives mentioned above, perylene bisimides combine the most important molecular features like planarity/rigidity, (photo)chemical and thermal stability, solubility, and structural versatility in a very advantageous way.[9] Consequently, the PBI π-system was systematically derivatized to create even more extended chromophores without compromising their superior properties. Thus, the *peri*-extension of perylene bisimides along its long molecular axis by insertion of additional naphthalene subunits results in higher homologue rylenes like terrylene (TBI) and quaterrylene

Received: June 30, 2016
Published: August 29, 2016

bisimides (QBI) with bathochromically shifted absorption maxima even in the near-infrared region.[10,11]

Likewise, the short molecular axis of perylene bisimides can easily be subjected to structural variations by introduction of additional substituents at the *ortho*- and *bay*-positions. However, *ortho*-functionalization has only been accomplished recently by different research groups using transition metal-catalyzed procedures to insert aliphatic or aromatic substituents as well as boronic acid ester functionalities.[12−15] These boronic acid esters provide additional access to a variety of substitution reactions such as halogenation, cyanation, or Suzuki−Miyaura cross-coupling for the construction of complex molecular architectures.[16,17] The *ortho*-modification indeed changes the optical and electronic properties of perylene bisimides without any significant impact on the planarity of the PBI π-system.[12,15] In contrast, the introduction of *bay*-substituents at the aromatic core directly influences the electronic structure of the PBI and causes contortion of the core. Depending on the size and the number of *bay*-substituents, the dihedral distortion strongly deviates from 0° to 35° like for tetra-brominated PBI-derivatives leading to (*P*) and (*M*) atropo-enantiomers.[18] In general, the *bay*-positions of perylene bisimides are prone to undergo chlorination, bromination, nitration, transition metal-mediated cross-coupling, or Diels−Alder reactions. The halogenated derivatives are of particular interest because these compounds can readily be used for nucleophilic substitutions or cross-coupling reactions.[9,19,20] Even core-annulated coronene-type derivatives as well as their azabenz-annulated analogues can be prepared starting from suitable *bay*-substituted PBI precursors.[21−23] These core-extended PBI derivatives are characterized by increased oscillator strength for the higher energetic S_0−S_2 transition because the respective transition dipole moment is aligned along the short molecular axis of the parent perylene core and rises with core extension.[5,6]

The optical, electronic, and structural properties of PBI derivatives can further be influenced by incorporating them via the *bay*-position as ligand systems into metal−organic complexes.[24−28] Only recently, we could demonstrate that core-extended azabenz-annulated perylene bisimides (abbreviated as ab-PBI) efficiently coordinate to ruthenium and iridium complex fragments.[29] The corresponding PBI transition metal complexes exhibit new and interesting optical properties like phosphorescence out of the PBI triplet state generated by spin−orbit coupling, which cannot be observed for the individual components. Therefore, we became highly interested in this exceptional class of PBI-based ligand systems and present now versatile protocols for the synthesis of azabenz-annulated perylene derivatives with different optical and electronic properties as well as variable coordination sites for the potential construction of multinuclear transition metal complexes.

■ RESULTS AND DISCUSSION

Monoazabenz-Annulated Perylene Derivatives with Symmetric *peri*-Substitution. The key step for the synthesis of all azabenz-annulated perylene derivatives presented in this work is the Pictet−Spengler (PS) reaction. Starting from amino-substituted perylene derivatives and the corresponding aldehydes, this Mannich-type transformation is initiated by an iminium ion formation followed by an intramolecular electrophilic aromatic substitution of the aromatic system by the iminium ion.[30] After annulation of the perylene core, an oxidative rearomatization takes place to generate the fully π-extended system.[31] The respective amino-functionalized perylene precursors can be obtained by well-established sequences of perylene core nitration (1- or 2-fold) and nitro group reduction to the amines.[32−34] However, for the synthesis of ab-PBIs **3a−f** (Scheme 1) containing up to three

Scheme 1. Synthesis of ab-PBIs 3a−f by Pictet−Spengler Reaction of Amino-PBI 1 with Different Aldehydes 2a−f

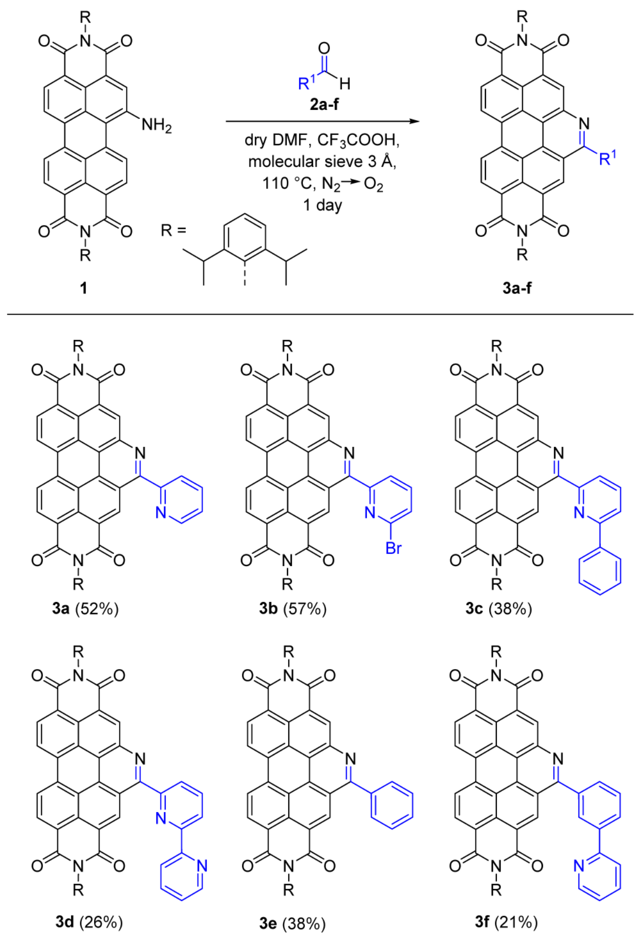

coordinating pyridyl subunits, we have developed a slightly modified procedure because the synthetic PS protocol described in the literature does not work for less reactive aldehydes.[22] Therefore, we (i) shifted the equilibrium of iminium ion formation toward the product by using dry *N*,*N*-dimethylformamide and adding molecular sieves to remove the released water; and (ii) after completion of iminium ion formation (∼30 min), the inert atmosphere was exchanged by pure oxygen to facilitate the oxidative rearomatization. Thus, ab-PBIs **3a−f** could be obtained in yields of up to 57%, which is remarkably high for such systems.

Whereas the functional properties of perylene bisimides are primarily encoded in the core substituents, the imide subunits are frequently used to manipulate properties like solubility or aggregation behavior in organic and aqueous media.[9] Usually, the synthesis of such customized imide substituents, which might be prone to oxidation, reduction, and/or labile under PS reaction conditions, is even more elaborate than that of the PBI itself, and the amount of material is often limited to a few milligrams. Therefore, we established an alternative synthetic procedure (Scheme 2) for the preparation of ab-PBIs bearing

DOI: 10.1021/acs.joc.6b01573
J. Org. Chem. 2016, 81, 8394−8405

Scheme 2. Synthetic Protocol for the Preparation of Azabenz-Annulated Perylene Bisanhydride ab-PBA 6 and Its Imidization Using the Customized Amine Derivative 7

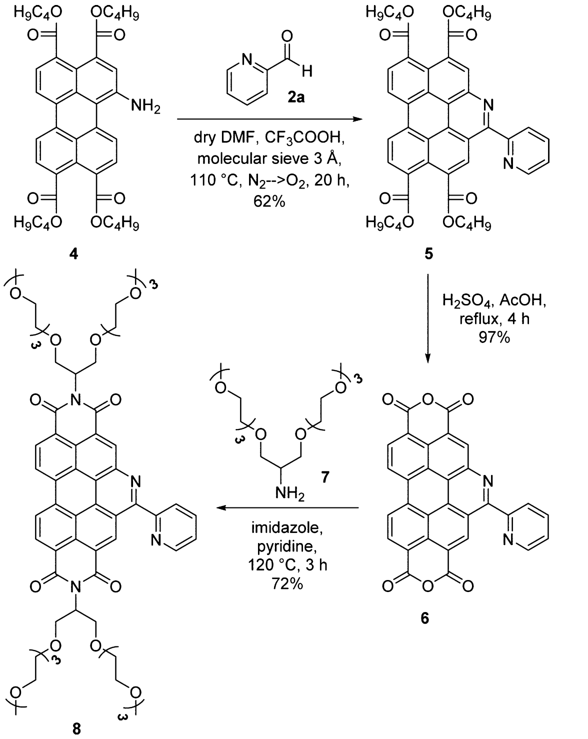

complex functional imide substituents in which the imidization is the final step of the entire synthetic route. The key intermediate of this pathway is the azabenz-annulated perylene bisanhydride (ab-PBA **6**), which constitutes a versatile starting material in this route. However, anhydride formation can be a tedious procedure starting from perylene bisimides (usually strong bases like KOH in refluxing alcohols are required) and is much more efficient from perylene tetraesters (usually organic acids in refluxing hydrocarbon solvents are utilized).[35,36] Thus, using the modified PS reaction protocol described above, we converted the literature-known amino-PTE **4**[37] with pyridine-2-carboxaldehyde **2a** into the bright-yellow ab-PTE **5** in 62% yield. Subsequently, the ester groups of **5** were hydrolyzed under acidic conditions to yield almost quantitatively the azabenz-annulated bisanhydride ab-PBA **6**. Like many other perylene bisanhydrides, **6** is nearly insoluble in all common organic solvents and is therefore difficult to characterize. However, ^{1}H and ^{13}C NMR spectroscopy in D_2SO_4 clearly proved the absence of any aliphatic proton with an appropriate number of aromatic signals for the protons of the perylene core and the pyridyl functionality.

An exemplary imidization reaction of ab-PBA **6** with an oligoethylene glycol-functionalized amine **7** was used to demonstrate the advantages of this synthetic pathway. After reacting **6** with 2 equiv of **7** in a mixture of molten imidazole and pyridine, the desired PBI **8** could be isolated in a good yield of 72%. Starting from commercially available perylene bisanhydride, this protocol illustrates even more convincingly its superiority by virtue of a total yield of 27% for compound **8** that drops down to an overall yield of only 2% using the conventional procedure described in Scheme 1.

Monoazabenz-Annulated Perylene Derivatives with Unsymmetric *peri*-Substitution. To extend the scope of such azabenz-annulated perylene derivatives, we developed a synthetic procedure for the preparation of unsymmetrically *peri*-substituted analogues like ab-perylene monoimide diester (PMIDE) **12**. These coordinating chromophores should be interesting starting materials for the fabrication of photoactive hybrid materials by attaching them to semiconducting surfaces like TiO_2. Accordingly, the regioselective nitration of unsymmetric perylene monoimide diester[38] (**9**, Scheme 3)

Scheme 3. Synthesis of Unsymmetric ab-PMIDE 12 and ab-PMIMA 13 by Regioselective Nitration and PS Transformation of PMIDE 9

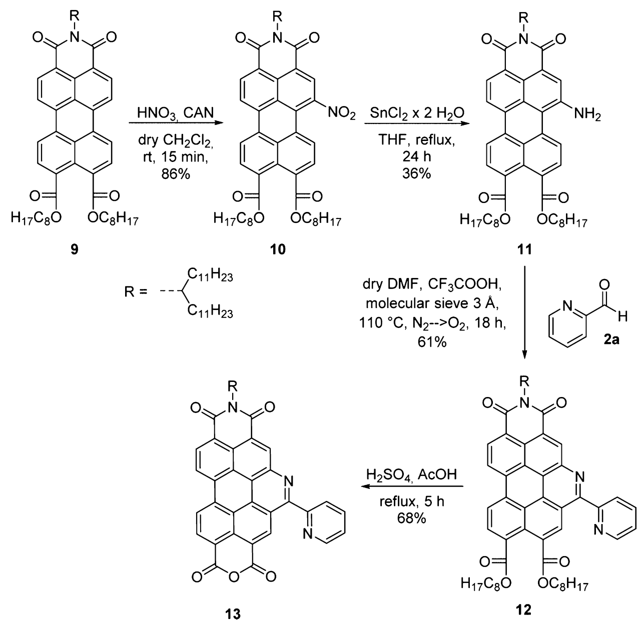

using cerium(IV)ammonium nitrate (CAN) and nitric acid as nitronium ion source yielded 1-nitro-PMIDE **10** in a very good yield of 86%.[39,40] Interestingly, under the applied reaction conditions (15 min at room temperature), only trace amounts of 2-fold nitrated byproducts could be detected by mass spectrometry.

Besides the high yield, an exclusive regioselectivity could be confirmed for the mononitrated 1-nitro-PMIDE **10** (for the numbering of the perylene core, see Figure 1) by 1D and 2D NMR spectroscopy (Figure 2 and Figure S1). It is important to note that the rotation of the "swallowtail" 12-tricosanyl ($CH(C_{11}H_{23})_2$) imide substituent around the C−N^{imide} bond is somewhat restricted at room temperature, giving rise to broad resonances for the protons at the 2 and 5 positions.[41] Although this signal broadening usually hampers the interpretation of NMR data, it can in this case be used as a sensitive probe for the correct assignment of the regioselectivity. Accordingly, for the 1-nitro-substituted PMIDE isomer, broad resonances can be detected for the hydrogen atoms at the 2 and 5 positions along with sharp doublets for the protons at the 6, 7, 8, 11, and 12 positions (see ^{1}H NMR trace in Figure 2), which exhibit appropriate $^{3}J_{HH}$ cross-signals. In contrast, for the corresponding 7-nitro-substituted regioisomer, a sharp singlet was expected for the hydrogen atom at the 8-position, which is clearly absent in the proton NMR spectrum. Further evidence is provided by two-dimensional correlation spectra (^{1}H,^{13}C-HMBC and ^{1}H,^{1}H-NOESY; see Figure S1) where cross-signals between H^8/H^{11} and the carbonyl carbon atoms in the ^{1}H,^{13}C-

DOI: 10.1021/acs.joc.6b01573
J. Org. Chem. 2016, 81, 8394−8405

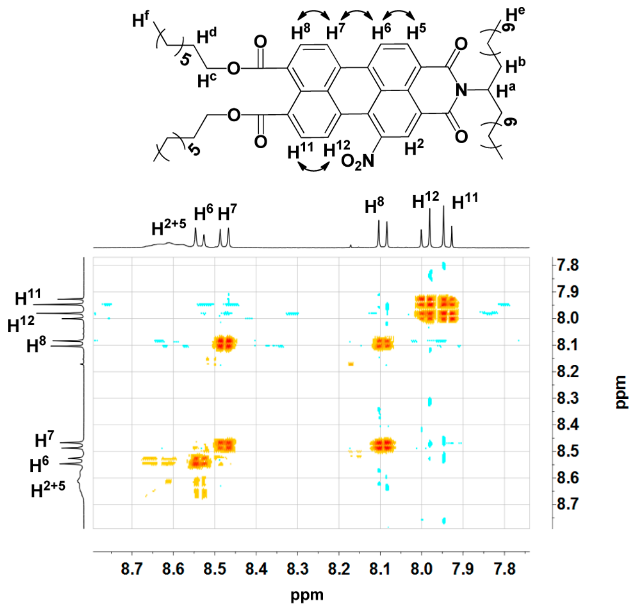

Figure 2. ^{1}H,^{1}H-COSY spectrum with assigned J_{HH} couplings of 1-nitro-PMIDE **10** in CD_2Cl_2 at room temperature (400 MHz). In the structure of **10** (above), the curved arrows indicate the cross coupling.

HMBC spectrum and between H^8/H^{11} and H^c in the ^{1}H,^{1}H-NOESY spectrum confirm the structural assignment.

After reduction of the nitro group using tin(II)chloride as reductant, 1-amino-PMIDE **11** was subjected to a PS transformation to obtain ab-PMIDE **12** in 61% yield. Subsequently, the ester functionalities of **12** were hydrolyzed under acidic conditions to generate the corresponding anhydride ab-perylene monoimide monoanhydride (PMIMA) **13**. Both diester **12** and particularly anhydride **13** are versatile starting materials for the preparation of unsymmetrically imide-substituted azabenz-annulated perylene bisimides and can additionally be used to anchor such dye molecules onto semiconducting surfaces.[42−44] All of these chromophores were fully characterized by ^{1}H and ^{13}C NMR spectroscopy, high-resolution mass spectrometry, and UV/vis spectroscopy, and their regioselective integrity was substantiated by 2D NMR spectroscopy.

Bisazabenz-Annulated Perylenes. While the azabenz-annulated perylene derivatives mentioned so far are capable of coordinating single transition metal centers, they do not provide access to multinuclear transition metal complexes with multiple redox active subunits and more sophisticated photophysics.[45−48] Therefore, we turned to bisazabenz-annulated systems, which have rarely been reported in the literature.[22] Starting from a 3:2 mixture of 1,7- and 1,6-diamino-substituted perylene bisimides (Scheme 4, left), *anti*-(ab)$_2$-PBI **15** and *syn*-(ab)$_2$-PBI **16**[22] are accessible by the PS protocol described above, and the regioisomers could be separated by column chromatography. Because of an elaborate purification process, both molecules were isolated in only moderate yields of 23% and 14%, respectively, pursuant to the isomeric ratio of the diamino-substituted precursor. Similarly, the bisazabenz-annulated perylene tetraester *syn*-(ab)$_2$-PTE **18** was synthesized by PS transformation of isomerically pure 1,6-diamino-PTE **17** in 37% yield (the corresponding 1,7-isomer could not be prepared as analytically pure material). After hydrolysis of **18**, the corresponding bisanhydride *syn*-(ab)$_2$-PBA **19** can be converted into bisazabenz-annulated perylene bisimides containing any desirable imide substituents (R) as illustrated by an imidization reaction using 2,6-diisopropylaniline as an example (Scheme 4, right).

Although *anti*-(ab)$_2$-PBI **15** and *syn*-(ab)$_2$-PBI **16** cannot be distinguished by high-resolution electron spray mass spectrometry, both isomers exhibit completely different dynamic behavior in solution as revealed by temperature-dependent

Scheme 4. Synthetic Access to Bisazabenz-Annulated Perylene Derivatives (ab)$_2$-PBI (left) and (ab)$_2$-PTE (right)

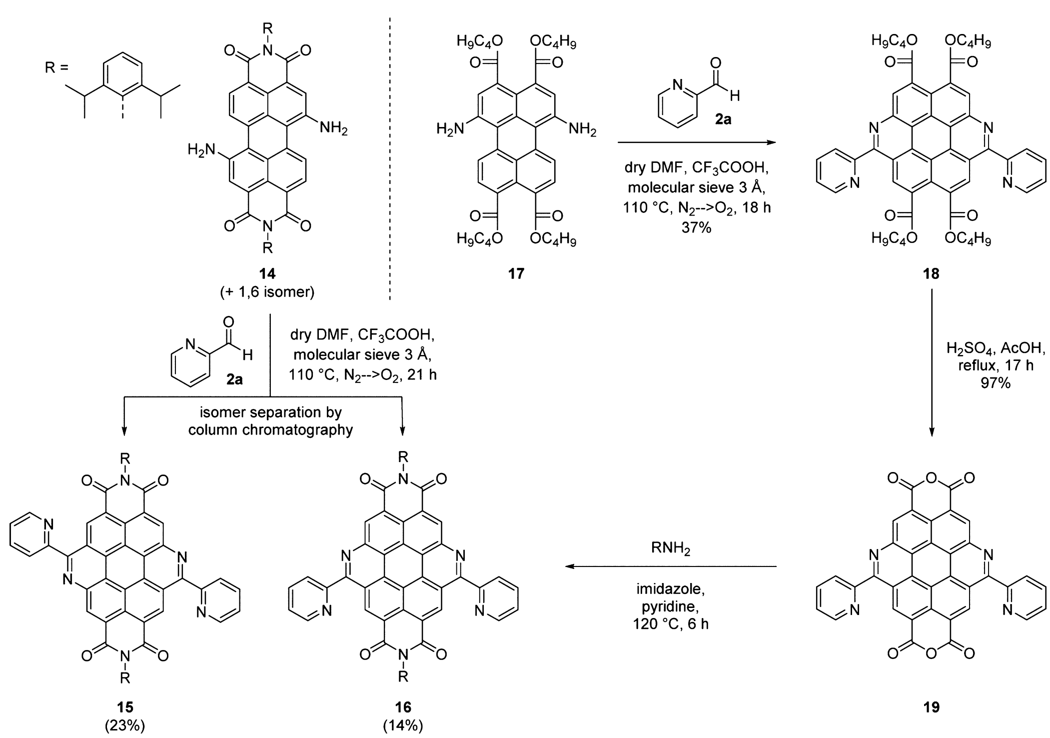

DOI: 10.1021/acs.joc.6b01573
J. Org. Chem. 2016, 81, 8394−8405

NMR spectroscopy in deuterated THF. Whereas *syn*-(ab)$_2$-PBI **16** is characterized by well-resolved NMR signals even at room temperature (295 K), only strongly broadened resonances are observed for *anti*-(ab)$_2$-PBI **15**, presumably due to the restricted rotation of the peripheral pyridine substituents that can efficiently be suppressed by protonation of the bipyridine subunits (see Figures S3 and S4). However, upon decreasing the temperature to 233 K, all aromatic resonances sharpened gradually, facilitating an unambiguous structural assignment.

Unequivocal structural evidence for the *anti*-bisazabenz-annulation in (ab)$_2$-PBI **15** is provided by X-ray diffraction experiments performed on single crystals grown from THF solutions (Figure 3). Apart from the *anti*-arrangement, (ab)$_2$-PBI **15** exhibits a completely flat aromatic core with both pyridyl substituents oriented out of the π-surface by 25° and 36°, respectively. Moreover, each bipyridine-like subunit is characterized by transoid oriented nitrogen atoms to minimize the electronic repulsion between the bipyridyl lone pairs. The length of the C−C bonds, which connect the pyridine substituents to the aromatic core (1.49 Å), is comparable with those of other 2,2′-bipyridine (~1.49 Å).[49] The whole single crystalline material is composed of well THF-solvated PBI dimers with less extended π−π-stacking due to the perpendicular oriented 2,6-diisopropylphenyl imide groups, which efficiently prevent columnar π−π-stacking arrangements.

(a)
(b)

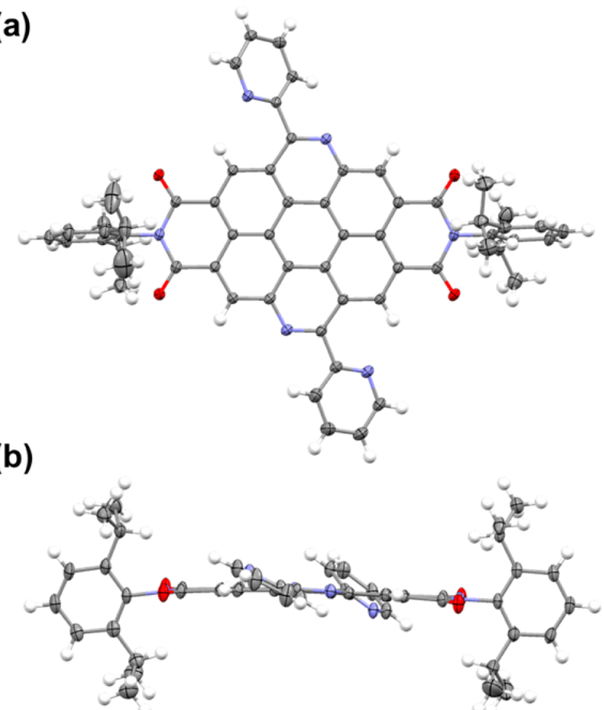

Figure 3. Molecular structure of *anti*-(ab)$_2$-PBI **15** in the solid state from top (a) and side views (b, ellipsoids set at 50% probability level; THF solvent molecules are omitted for clarity).

Optical and Redox Properties of ab-Perylene Derivatives. The variety of different azabenz-annulated perylene derivatives accomplished in this work enables a systematic comparison of their optical and redox properties (see Table 1). Two distinct effects can thus be studied based on this library of compounds: (i) the effect of perylene core extension (1- and 2-fold) along the short molecular axis; and (ii) the influence of the *peri*-substituents (imide, anhydride, and ester functionalities) on the optoelectronic properties of monoazabenz-annulated perylenes. Because the variation of the terminal substituents does not significantly influence the optical properties of the individual chromophores, these data were exclusively summarized in Table S1.

Obviously, upon core extension, a hypsochromic shift of the S_0−S_1 transition band, referred to the parent PBI, can be observed that is less pronounced for the bisazabenz-annulated PTE **18** and its PBI analogues **15** and **16** (see Figure 4a and Figure S5 (top)). Simultaneously, the oscillator strengths and the intensities of the S_0−S_2 transitions strongly increase with core extension because the S_0−S_2 transition dipole moments are aligned along the laterally elongated molecular axes. Therefore, the UV/vis absorption spectra of *syn*-(ab)$_2$-PTE **18**, *syn*-(ab)$_2$-PBI **16**, and *anti*-(ab)$_2$-PBI **15** are not predominated anymore by the lowest energy S_0−S_1 transitions but by higher energy absorption bands with extinction coefficients of up to ε = 119 × 10^3 M^{-1} cm^{-1}. Similar observations (hypsochromic shift of the absorption maxima and intensification of the S_0−S_2 transition) have already been reported by the groups of Nijegorodov, Adachi, and Müllen for core-extended perylene derivatives (Nijegorodov, perylene, 1,12-benzoperylene, and coronene; Adachi and Müllen, perylene bisimide, benzo[*g*,*h*,*i*]-perylene bisimide, and coronene bisimide).[5,50,51] However, for the monoazabenz-annulated compounds ab-PBI **3a**, ab-PMIMA **13**, ab-PMIDE **12**, and ab-PTE **5**, the S_0−S_1 transitions (longitudinally polarized along the N−N molecular axes) still exhibit enough oscillator strength, giving rise to intensive lowest energy absorption bands with well-resolved vibronic progressions (Figure 4b). Both chromophores **3a** and **13** have nearly the same conjugation length and are therefore characterized by similar absorption spectral features with a minor spectral shift of only 6 nm that can be ascribed to slightly different electronic properties (vide infra). However, the size of the fully π-conjugated system is gradually reduced from ab-PBI **3a** to ab-PMIDE **12** and ab-PTE **5**, resulting in hypsochromically shifted absorption spectra with lowest energy UV/vis transitions located at 475, 454, and 430 nm, respectively. Thus, a blue-shift of approximately 23 nm per introduced diester functionality can be ascertained for the S_0−S_1 transitions with nearly unaffected higher energetic UV/vis absorptions. All present perylene derivatives exhibit fluorescence emission out of the first excited singlet state with mirror image like vibronic fine structures and comparatively small Stokes shifts (see Figure S6). However, azabenz-annulation causes the fluorescence quantum yield to be quenched by 30−40% per azabenz-annulation due to decreasing oscillator strengths of the S_1−S_0 transitions (vide supra).[52] Therefore, the bright fluorescence of PTE and PBI (quantum yields close to unity) is reduced to 41−69% for monoazabenz-annulated chromophores and diminishes to 9−23% for the bisazabenz-annulated derivatives (see Table 1). Likewise, protonation of the azabenz-annulated chromophores with trifluoroacetic acid gradually quenches the emission, as it has exemplarily been demonstrated for ab-PBI **3a** (see Figure S7).

To experimentally assess the energies of the frontier molecular orbitals as a function of perylene core extension and *peri*-substitution, we determined the reduction potentials of the individual chromophores by cyclic voltammetry in dichloromethane using *n*-Bu_4NPF_6 as electrolyte and ferrocene as internal standard (see Table 1). Apparently, upon core annulation, both reduction processes $E_{1/2}^{\text{first red}}$ and $E_{1/2}^{\text{second red}}$ become gradually shifted to more negative values. Accordingly,

DOI: 10.1021/acs.joc.6b01573
J. Org. Chem. 2016, 81, 8394−8405

Table 1. Summary of the Optical and Redox Data of Different Azabenz-Annulated Perylene Derivative Series[a]

	λ_{abs}/nm (ε/10^3 M^{-1} cm^{-1})		λ_{em}/nm					
compounds	S_0-S_1	S_0-S_x	S_1-S_0	Φ_F	$E_{1/2}^{first\ red}$/V[b]	$E_{1/2}^{second\ red}$/V[b]	E^{LUMO}/eV[c]	E^{HOMO}/eV[d]
PTE	471 (40.6)	353 (2.4)	486	0.98	−1.54	−1.79	−3.26	−5.85
ab-PTE (**5**)	430 (25.7)	319 (43.4)	440	0.41	−1.60	−1.88	−3.20	−6.06
syn-(ab)$_2$-PTE (**18**)	445 (1.8)	336 (119)	450	0.09	−1.68	−1.98	−3.12	−5.89
PBI	527 (94.7)	370 (5.8)	532	0.96	−0.99	−1.22	−3.91	−6.25
ab-PBI (**3a**)	475 (68.4)	333 (29.2)	484	0.69	−1.06	−1.34	−3.74	−6.33
anti-(ab)$_2$-PBI (**15**)	485 (20.5)	354 (85.0)	493	0.23	−1.13	−1.43	−3.67	−6.21
syn-(ab)$_2$-PBI (**16**)	478 (4.8)	355 (83.0)	485	0.22	−1.16	−1.44	−3.64	−6.21
ab-PBI (**3a**)[e]	475 (68.4)	333 (29.2)	484	0.69	−1.06	−1.34	−3.74	−6.33
ab-PMIMA (**13**)	469 (41.7)	322 (33.4)	478	0.50	−1.05	−1.31	−3.75	−6.37
ab-PMIDE (**12**)	454 (36.9)	318 (32.3)	468	0.77	−1.35	−1.64	−3.45	−6.15
ab-PTE (**5**)[e]	430 (25.7)	319 (43.4)	440	0.41	−1.60	−1.88	−3.20	−6.06

[a]Measured in dichloromethane at 298 K. [b]Measured with 0.1 M n-Bu$_4$NPF$_6$ and with Fc^+/Fc as a reference. [c]Energy of the lowest unoccupied molecular orbital E^{LUMO} in eV as calculated considering the energy level of Fc^+/Fc with respect to the vacuum level by using $E^{LUMO} = [-(E_{1/2}^{first\ red}) - 4.8]$ eV. [d]Energy of the highest occupied molecular orbital E^{HOMO} in eV was calculated by using $E^{HOMO} = [E^{LUMO} - E^{opt.gap}]$; $E^{opt.gap}$ determined at the intersection of the absorption and emission spectra with the latter being normalized with respect to the lowest-energy absorption. [e]For the sake of clarity, the data are repeated for comparison.

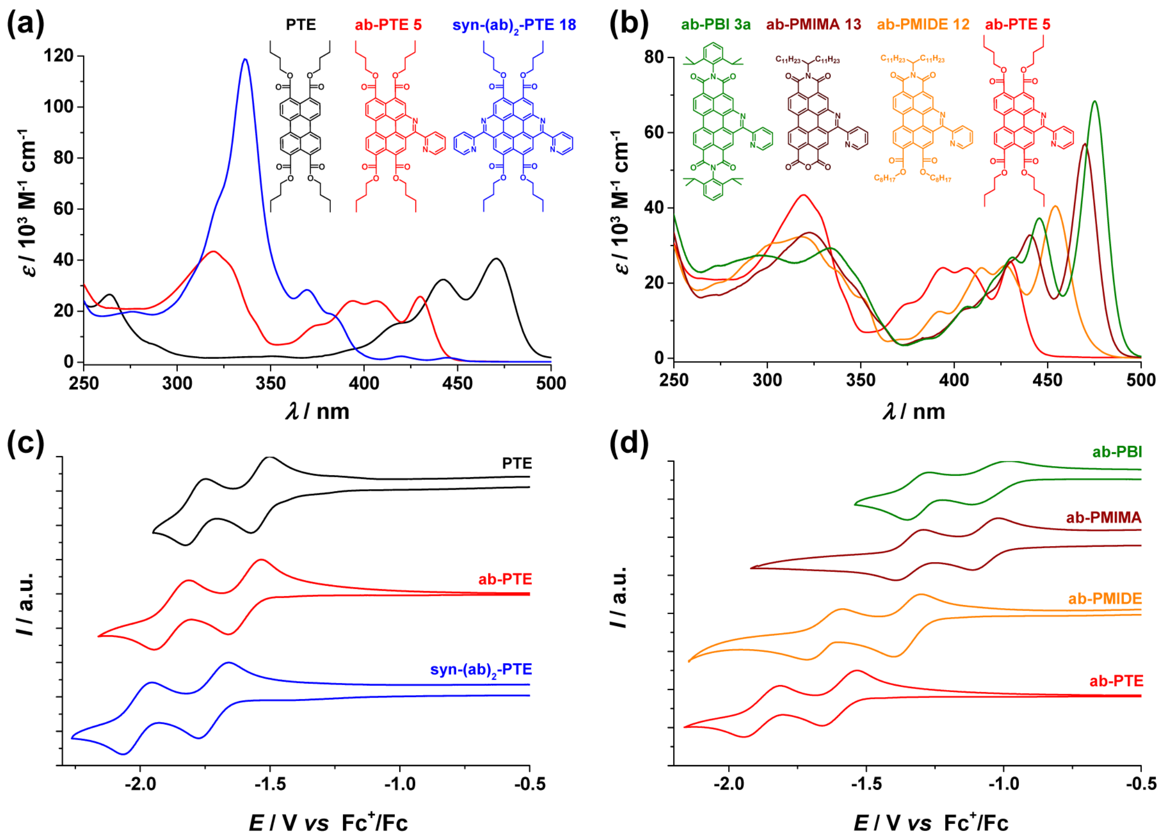

Figure 4. UV/vis absorption spectra (c = 1 × 10^{-5} M) of the core-extended perylene tetraester series (a) and of the monoazabenz-annulated perylenes derivative series (b). Cyclic voltammograms (c = 2.5 × 10^{-4} M, electrolyte: 0.1 M n-Bu$_4$NPF$_6$) of the core-extended perylene tetraester series (c) and of the monoazabenz-annulated perylene derivative series (d). The electrochemical values were corrected versus ferrocenium/ferrocene (Fc^+/Fc) as an internal standard. All measurements were performed in dichloromethane at room temperature.

azabenz-annulation disfavors reduction to mono- and dianionic species as it becomes evident by comparing both the PTE (PTE, ab-PTE **5**, *syn*-(ab)$_2$-PTE **18**; see Figure 4c) and the PBI series (PBI, ab-PBI **3a**, *anti*-(ab)$_2$-PBI **15**, *syn*-(ab)$_2$-PBI **16**; see Figure S5 (bottom)). In contrast, the reduction potentials of the monoazabenz-annulated systems are highly dependent on the electron-accepting properties of the respective *peri*-substituents. Thus, with an increasing number of coplanar electron-withdrawing subunits (ab-PTE **5** < ab-PMIDE **12** < ab-PMIMA **13** ≈ ab-PBI **3a**; see Figure 4d), the two reduction processes are gradually shifted to more positive potentials. Altogether, an electrochemical window of 690 and 760 mV for the first and second reduction, respectively, can be covered by this library of azabenz-annulated perylene derivatives.

Energies of Frontier Molecular Orbitals and DFT Calculations. Considering the energy level of ferrocenium/

DOI: 10.1021/acs.joc.6b01573
J. Org. Chem. 2016, 81, 8394−8405

ferrocene (Fc^+/Fc) with respect to the vacuum level (−4.8 eV), the LUMO levels of the azabenz-annulated perylene derivatives can readily be estimated using their experimentally determined reduction potentials according to $E^{\mathrm{LUMO}} = -[E_{1/2}^{\mathrm{first\ red}} + 4.8]$ eV (see Table 1). The order of the LUMO energies thus obtained is well reproduced by our DFT calculations on a B3LYP/def2SVP level of theory (Figure 5, black and gray marks). The energetic offset of up to 0.5 eV can presumably be ascribed to solvent effects, which were not implemented in our theoretical considerations.

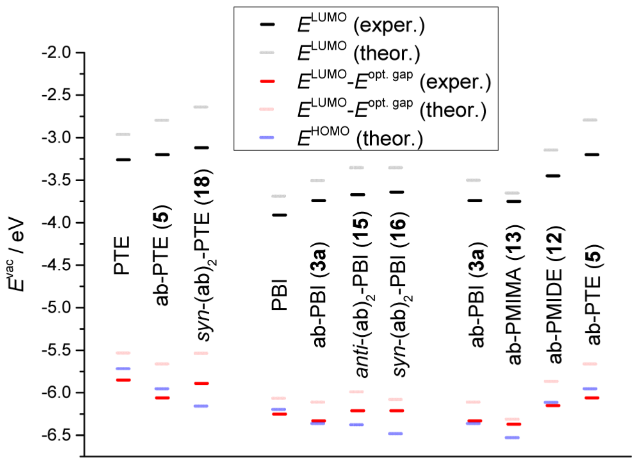

Figure 5. Schematic representation of the frontier molecular orbital energies of azabenz-annulated perylene derivatives. The experimentally determined values are obtained from electrochemical and absorption properties (see Table 1). The theoretical data are based on DFT calculations at the B3LYP/Def2SVP level of theory (for details, see the Supporting Information).

In contrast, the HOMO levels of these chromophores could not be estimated by following the same approach because the oxidation potentials of many derivatives are not covered by the electrochemical window of our experimental setup. However, on the basis of the assumption that the lowest energetic optical transition directly reflects the HOMO−LUMO energy gap, the HOMO energies should in principle be accessible by subtracting the optical band gap from the respective LUMO level ($E^{\mathrm{HOMO}} = E^{\mathrm{LUMO}} - E^{\mathrm{opt.gap}}$, Table 1 and Figure 5, red marks). Although the energetic order of these values is in good agreement with the corresponding ones obtained by DFT methods (Figure 5, pink marks), there is an obvious deviation from the directly calculated values (Figure 5, blue marks). This divergence can be explained by the fact that especially for the bisazabenz-annulated perylene derivatives, transitions between other molecular orbitals like HOMO−1 and LUMO+1 contribute to the lowest energetic UV/vis absorption (see Table S2).

■ CONCLUSION

In summary, we presented here synthetic approaches for the preparation of different azabenz-annulated perylene derivatives possessing versatile functionalities. These include (i) polypyridyl core-substituted monoazabenz-annulated compounds as chelating ligands with different binding modes, (ii) perylene bisanhydrides like ab-PBA **6** and *syn*-(ab)$_2$-PBA **19**, which serve as universal starting materials for the construction of azabenz-annulated perylene bisimides with complex and highly functionalized imide substituents, (iii) regioisomers of ab-perylene monoimide monoanhydride (ab-PMIMA **13**) and ab-perylene monoimide diester (ab-PMIDE **12**), which can be used either for the fabrication of unsymmetrically substituted ab-perylene bisimides or for anchoring such chromophores on semiconducting surfaces, and (iv) bisazabenz-annulated derivatives for the preparation of even multinuclear transition metal complexes. A comprehensive characterization of their molecular properties by NMR and optical spectroscopy, cyclic voltammetry, high-resolution mass spectrometry, and single-crystal structure analysis, in combination with DFT calculations, revealed that the optical and electronic properties of these multifunctional chromophores can readily be adjusted to many desirable applications by ligation on surfaces, for example, TiO_2, or coordination to transition metals.[29,42] Accordingly, our current efforts are directed to implement these promising ligands as integral components into hybrid materials for the construction of photoredox catalysts, which will be reported in due course.

■ EXPERIMENTAL SECTION

Materials and Methods. *N,N′*-Bis(2′,6′-diisopropylphenyl)-1-amino-perylene-3,4:9,10-tetracarboxylic acid bisimide (**1**, amino-PBI),[34] a 1,6- and 1,7-isomeric mixture of *N,N′*-bis(2′,6′-diisopropylphenyl)-diamino-perylene-3,4:9,10-tetracarboxylic acid bisimide (**14**, 1,7- and 1,6-diamino-PBI),[34] 1-amino-perylene-3,4,9,10-tetracarboxylic acid tetrabutyl ester (**4**, amino-PTE),[37] 1,6-diamino-perylene-3,4,9,10-tetracarboxylic acid tetrabutyl ester (**17**, 1,6-diamino-PTE),[37] *N*-(12′-tricosanyl)-perylene-3,4-dicarboxylic acid monoimide-9,10-dicarboxylic acid dioctyl ester (**9**, PMIDE),[38] 6-phenyl-pyridine-2-carboxaldehyde (**2c**),[53] 6-pyridin-2′-yl-pyridine-2-carboxaldehyde (**2d**),[54] and 2,5,8,11,15,18,21,24-octaoxapentacosan-13-amine (**7**)[55,56] were synthesized according to literature known procedures. All other starting materials were purchased from commercial sources and used as obtained, unless otherwise noted. Dichloromethane and *N,N*-dimethylformamide were dried with a commercial solvent purification system. Column chromatographic separations were performed on silica gel 60 M (0.04−0.063 mm). For thin-layer chromatography (TLC) aluminum sheets precoated with silica gel 60 F254 were used. Preparative size-exclusion chromatography was performed using a styrene-based material (mesh size, 200−400; molar mass operation range, up to 2000 g/mol) swollen with dichloromethane/methanol 9:1. NMR spectra were recorded on a 400 MHz NMR spectrometer in deuterated solvents at 25 °C. Chemical shifts are reported in parts per million (ppm, δ scale) relative to the signal of the residual undeuterated solvent. The following abbreviations were used to describe nuclear spin coupling: s = singlet, d = doublet, t = triplet, sept = septet, m = multiplet, and b = broad. Melting points were determined on a commercial polarization microscope and are uncorrected. MALDI-ToF MS spectra were measured with commercial spectrometers either in the positive or in the negative reflector mode using *trans*-2-[3-(4-*tert*-butylphenyl)-2-methyl-2-propenylidene]malononitrile (DCTB) as a matrix. In addition, high-resolution mass spectra (ESI) were recorded on a standard mass spectrometer with a time-of-flight detector. UV/vis absorption spectra were measured on a commercial UV/vis spectrophotometer at 20 °C by using 1 cm quartz cuvettes in dichloromethane as solvent (spectroscopy grade). Emission spectra were recorded on a commercial fluorescence spectrophotometer at 20 °C in 1 cm quartz cuvettes as dichloromethane (spectroscopy grade) solutions, which had a maximal absorbance of less than 0.05. The quantum yields were determined using a commercial absolute quantum yield measurement system. The system is composed of an excitation source that uses a 150 W CW xenon light source, a monochromator (250−700 nm, fwhm 10 nm), an integrating sphere, and a multichannel spectrometer capable of simultaneously measuring multiple wavelengths between 300 and 950 nm and counting the number of absorbed and emitted photons. The reported quantum yields are averaged from values

DOI: 10.1021/acs.joc.6b01573
J. Org. Chem. 2016, 81, 8394−8405

measured at three different excitation wavelengths. Electrochemical measurements were performed on a commercial instrument with a standard three-electrode configuration; scan rates from 20 to 1000 mV/s were applied. The experiments were carried out in dry (distillation over CaH_2) and degassed dichloromethane at a concentration of 2.5×10^{-4} M containing tetra-*n*-butylammonium hexafluorophosphate (0.1 M) as electrolyte. Ferrocene (Fc) was added at the end of each experiment as an internal standard. The potentials are referred to the ferrocenium/ferrocene couple (Fc^+/Fc). All computational calculations were performed using the Gaussian 09 program package.[57] The DFT calculations were carried out with B3LYP[58−60] as functional and def2-SVP[61] as basis set. The structures were geometry optimized, followed by frequency calculations on the optimized structures, which confirmed the existence of an energy minimum. Time-dependent (TD)-DFT calculations were carried out on the optimized structure with the lowest energy of the compounds using the same functional (B3LYP) and basis set (def2-SVP) as for the geometry optimization. The data are summarized in Tables S2−S12. Long alkyl chains were replaced by ethyl groups to simplify and thus accelerate the calculations.

X-ray Crystal Structure Determination. Single-crystal X-ray diffraction data for *anti*-(ab)$_2$-PBI **15** were collected at 100 K on a commercial diffractometer using multilayered mirror monochromated Cu K_α radiation. The structures were solved using direct methods, expanded with Fourier techniques, and refined with a standard software package.[62] All non-hydrogen atoms were refined anisotropically. Hydrogen atoms were included in the structure factor calculation on geometrically idealized positions. Single crystals of *anti*-(ab)$_2$-PBI **15** suitable for X-ray structural analysis were grown by slow evaporation of a concentrated solution of tetrahydrofuran (THF). The single crystals thus obtained were highly sensitive toward temperature. Therefore, the crystalline material was directly immersed (in solution) into a film of perfluorpolyether, which was precooled to 200 K on a copper substrate. Subsequently, the investigated single crystal was transferred on a Teflon loop to the diffractometer continuously cooled by evaporated liquid nitrogen. The refinement showed at least two more disordered THF molecules, which could not be modeled satisfactorily. Therefore, the SQUEEZE routine of PLATON was used to remove the electron density. The remaining structure could be refined nicely.[63]

Crystal data for *anti*-(ab)$_2$-PBI **15** ($C_{60}H_{46}N_6O_4 \cdot 4C_4H_8O$): M_r = 1203.44, 0.34 × 0.23 × 0.19 mm^3, triclinic space group $P\bar{1}$, a = 10.9630(5) Å, α = 97.6970(16)°, b = 18.4513(8) Å, β = 97.8872(16)°, c = 33.0607(14) Å, γ = 100.9697(16)°, V = 6414.6(5) Å^3, Z = 4, ρ(calcd) = 1.246 g cm^{-3}, μ = 0.646 mm^{-1}, $F_{(000)}$ = 2560, GOF(F^2) = 1.065, R_1 = 0.0809, wR_2 = 0.2239 for $I > 2\sigma(I)$, R_1 = 0.0895, wR_2 = 0.2313 for all data, 25 241 unique reflections [$\theta \leq 72.817°$] with a completeness of 99.6% and 1707 parameters, 208 restraints.

Crystallographic data have been deposited with the Cambridge Crystallographic Data Centre as supplementary publication no. CCDC 1489244. These data can be obtained free of charge from the Cambridge Crystallographic Data Centre via www.ccdc.ac.uk/data.request/cif.

General Procedure of the Pictet−Spengler Reaction for Azabenz-Annulation. The mono- or diamino-perylene derivative (1 equiv), the respective aromatic aldehyde (4−20 equiv), and activated molecular sieve (3 Å) were placed in a Schlenk flask. Afterward, dry dimethylformamide (10 mL per 100 mg of amino-perylene derivative) and trifluoroacetic acid (10 equiv) were added under inert conditions, and the reaction mixture was stirred at 110 °C for 30 min under nitrogen atmosphere. Subsequently, the inert atmosphere was replaced by pure oxygen, and the reaction mixture was stirred under this oxidative environment at 110 °C until a full conversion of amino-perylene (monitored by TLC). The mixture was quenched by addition of water and neutralized with 15% sodium hydroxide solution. After extraction with dichloromethane, the organic layer was washed twice with brine and twice with water. The crude product was further purified by column chromatography and recrystallization.

In the following, a general structure of azabenz-annulated PBI (ab-PBI) is depicted with indexing of atom and bond positions applied in the nomenclature of the compounds.

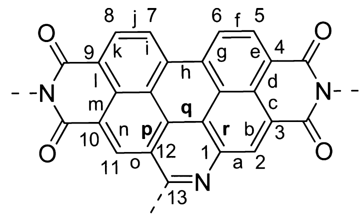

*N,N′-Bis(2′,6′-diisopropylphenyl)-13-(pyridin-2″-yl)-azabenzo[pqr]-perylene-3,4:9,10-tetracarboxylic Acid Bisimide (ab-PBI, **3a**).* The reaction was performed according to the general Pictet−Spengler reaction procedure using 0.74 g (1.02 mmol) of amino-PBI **1** and 0.72 g (6.72 mmol) of pyridine-2-carboxaldehyde **2a**. The product was obtained as a yellow solid after column chromatography (SiO_2, EtOAc/hexane 1:2) and recrystallization (EtOAc). The analytical data are in agreement with those described in the literature.[22] Yield: 0.43 g (0.53 mmol, 52%). Mp > 300 °C. ^{1}H NMR (400 MHz, CD_2Cl_2): δ = 10.52 (s, 1H), 9.63 (s, 1H), 9.45−9.40 (m, 2H), 9.22−9.18 (m, 2H), 8.96−8.94 (m, 1H), 8.62 (ddd, ^3J = 7.9 Hz, ^4J = 1.2 Hz, ^5J = 0.8 Hz, 1H), 8.13 (td, ^3J = 7.8 Hz, ^4J = 1.8 Hz, 1H), 7.62−7.55 (m, 3H), 7.44−7.41 (m, 4H), 2.90 (sept, ^3J = 6.7 Hz, 4H), 1.24−1.19 (m, 24H). ^{13}C NMR (100 MHz, CD_2Cl_2): δ = 164.3, 164.20, 164.20, 164.1, 157.90, 157.87, 149.4, 146.54, 146.52, 144.5, 138.0, 135.7, 135.12, 135.09, 133.9, 131.51, 131.47, 131.45, 130.5, 130.4, 130.1, 130.0, 129.1, 127.7, 126.8, 126.3, 124.73, 124.68, 124.6, 124.5, 124.1, 123.9, 123.6, 123.4, 122.8, 122.7, 120.1, 29.7, 29.6, 24.23, 24.20, 24.16. MS (MALDI-TOF, matrix, DCTB; mode, negative): m/z calcd for $[C_{54}H_{44}N_4O_4]^-$ 812.3; found 812.0. HRMS (ESI-TOF, positive, acetonitrile/chloroform): m/z $[M + H]^+$ calcd for $[C_{54}H_{45}N_4O_4]^+$ 813.3441; found 813.3435 (error = 0.2 ppm). UV/vis (CH_2Cl_2, nm): λ_{max} (ε_{max} M^{-1} cm^{-1}) = 475 (68 400), 445 (37 200), 431 (26 900), 334 (29 300). CV (CH_2Cl_2, 0.1 M TBAPF$_6$, V vs Fc^+/Fc): $E_{1/2}$ = −1.06 (PBI$^{-/0}$), −1.34 (PBI$^{2-/-}$).

*N,N′-Bis(2′,6′-diisopropylphenyl)-13-(6″-bromopyridin-2″-yl)-azabenzo[pqr]-perylene-3,4:9,10-tetracarboxylic Acid Bisimide (**3b**).* The reaction was performed according to the general Pictet−Spengler reaction procedure using 0.70 g (0.964 mmol) of amino-PBI **1** and 1.0 g (5.36 mmol) of 6-bromo-pyridine-2-carboxaldehyde **2b**. The product was obtained as a yellow solid after column chromatography (SiO_2, EtOAc/hexane 1:2) and recrystallization (MeOH). Yield: 0.49 g (0.55 mmol, 57%). Mp > 300 °C. ^{1}H NMR (400 MHz, CD_2Cl_2): δ = 10.66 (s, 1H), 9.69 (s, 1H), 9.53−9.49 (m, 2H), 9.28 (d, ^3J = 8.1 Hz, 1H), 9.24 (d, ^3J = 8.1 Hz, 1H), 8.69 (dd, ^3J = 7.7 Hz, ^4J = 0.8 Hz, 1H), 8.04 (t, ^3J = 7.8 Hz, 1H), 7.83 (dd, ^3J = 7.9 Hz, ^4J = 0.8 Hz, 1H), 7.64−7.59 (m, 2H), 7.48−7.45 (m, 4H), 2.98−2.90 (m, 4H), 1.27−1.13 (m, 24H). ^{13}C NMR (100 MHz, CD_2Cl_2): δ = 163.9, 163.8, 163.74, 163.69, 158.0, 155.2, 146.13, 146.11, 144.0, 140.9, 140.0, 135.3, 134.7, 134.0, 133.6, 131.2, 131.1, 131.0, 130.2, 130.1, 129.7, 129.6, 128.8, 128.7, 127.4, 126.0, 125.1, 124.4, 124.20, 124.18, 124.1, 124.0, 123.5, 123.2, 123.1, 122.4, 122.3, 120.0, 29.3, 23.81, 23.78, 23.76. MS (MALDI-TOF, matrix, DCTB; mode, negative): m/z calcd for $[C_{54}H_{43}BrN_4O_4]^-$ 890.25; found 890.19. HRMS (ESI-TOF, positive, methanol/chloroform): m/z $[M + H]^+$ calcd for $[C_{54}H_{44}BrN_4O_4]^+$ 891.2540; found 891.2540 (error = 0.1 ppm). UV/vis (CH_2Cl_2, nm): λ_{max} (ε_{max} M^{-1} cm^{-1}) = 473 (66 200), 443 (36 300), 432 (27 500), 407 (14 100), 337 (30 400).

*N,N′-Bis(2′,6′-diisopropylphenyl)-13-(6″-phenyl-pyridin-2″-yl)-azabenzo[pqr]-perylene-3,4:9,10-tetracarboxylic Acid Bisimide (**3c**).* The reaction was performed according to the general Pictet−Spengler reaction procedure using 0.29 g (0.40 mmol) of amino-PBI **1** and 0.48 g (2.62 mmol) of 6-phenyl-pyridine-2-carboxaldehyde **2c**. The product was obtained as a yellow solid after column chromatography (SiO_2, EtOAc/hexane 1:2) and recrystallization (EtOAc). Yield: 134 mg (0.15 mmol, 38%). Mp > 300 °C. ^{1}H NMR (400 MHz, CD_2Cl_2): δ = 10.90 (s, 1H), 9.59 (s, 1H), 9.39−9.37 (m, 2H), 9.16 (d, ^3J = 8.3 Hz, 1H), 9.08 (d, ^3J = 8.1 Hz, 1H), 8.59 (dd, ^3J = 7.8 Hz, ^4J = 0.9 Hz, 1H), 8.22–8.20 (m, 2H), 8.11 (t, ^3J = 7.9 Hz, 1H), 7.97 (dd, ^3J = 7.9 Hz, ^4J = 0.8 Hz, 1H), 7.49 (t, ^3J = 7.9 Hz, 2H), 7.42–7.33 (m, 7H), 2.83 (sep, ^3J = 6.8 Hz, 4H), 1.17–1.12 (m, 24H). ^{13}C NMR (100 MHz, CD_2Cl_2): δ = 164.1, 163.93, 163.86, 163.8, 157.2, 157.1, 157.0, 146.2, 146.1, 144.1, 138.9, 138.5, 135.5, 135.2, 134.8, 133.5, 131.2, 131.12, 131.07, 130.3, 130.0, 129.7, 129.6, 129.3, 128.9, 128.8, 127.3, 127.2, 125.9, 124.7, 124.4, 124.2, 123.8, 123.7, 123.5, 123.0, 122.4, 122.3, 121.0, 119.9, 29.29, 29.26, 23.9, 23.82, 23.77, 23.7. MS (MALDI-TOF, matrix, DCTB; mode, positive): m/z calcd for $[C_{60}H_{48}N_4O_4]^+$ 888.37; found 887.96. HRMS (ESI-TOF, positive, acetonitrile/chloroform): m/z $[M + H]^+$ calcd for $[C_{60}H_{49}N_4O_4]^+$ 889.3748; found 889.3751 (error = 0.3 ppm). UV/vis (CH_2Cl_2, nm): λ_{max} (ε_{max} M^{-1} cm^{-1}) = 478 (61 700), 448 (34 100), 433 (29 400), 338 (33 900). CV (CH_2Cl_2, 0.1 M $TBAPF_6$, V vs Fc^+/Fc): $E_{1/2}$ = −1.08 ($PBI^{-/0}$), −1.36 ($PBI^{2-/-}$).

*N,N′-Bis(2′,6′-diisopropylphenyl)-13-(2″,2‴-bipyridin-6″-yl)-azabenzo[pqr]-perylene-3,4:9,10-tetracarboxylic Acid Bisimide (**3d**).* The reaction was performed according to the general Pictet–Spengler reaction procedure using 40 mg (0.07 mmol) of amino-PBI **1** and 92 mg (0.50 mmol) of 6-pyridin-2′-yl-pyridine-2-carboxaldehyde **2d**. The product was obtained as a yellow solid after column chromatography (SiO_2, 99:1 CH_2Cl_2/MeOH) and precipitation (CH_2Cl_2 in n-hexane). Yield: 16 mg (18 μmol, 26%). Mp > 300 °C. ^{1}H NMR (400 MHz, CD_2Cl_2): δ = 10.98 (s, 1H), 9.62 (s, 1H), 9.42–9.40 (m, 2H), 9.18 (d, ^3J = 8.2 Hz, 1H), 9.11 (d, ^3J = 8.2 Hz, 1H), 8.74 (dd, ^3J = 7.8 Hz, ^4J = 1.0 Hz, 1H), 8.66–8.62 (m, 3H), 8.18 (t, ^3J = 7.9 Hz, 1H), 7.68 (td, ^3J = 7.6 Hz, ^4J = 2.0 Hz, 1H), 7.52–7.47 (m, 2H), 7.36–7.34 (m, 4H), 7.26 (ddd, ^3J = 7.5 and 4.7 Hz, ^4J = 1.1 Hz, 1H), 2.83 (sep, ^3J = 6.9 Hz, 4H), 1.15–1.12 (m, 24H). ^{13}C NMR (100 MHz, CD_2Cl_2): δ = 164.3, 164.1, 164.0, 163.9, 156.9, 156.8, 155.9, 155.7, 149.4, 146.3, 146.2, 144.3, 138.8, 137.3, 135.7, 135.4, 135.0, 133.7, 131.3, 131.2, 130.5, 130.2, 129.82, 129.78, 129.0, 127.5, 126.4, 126.0, 124.5, 124.4, 124.2, 124.0, 123.8, 123.7, 123.5, 123.2, 122.6, 122.4, 121.8, 121.4, 120.1, 29.42, 29.40, 24.1, 24.0, 23.9, 23.8. MS (MALDI-TOF, matrix, DCTB; mode, positive): m/z calcd for $[C_{59}H_{47}N_5O_4]^+$ 889.36; found 889.29. HRMS (ESI-TOF, positive, acetonitrile/chloroform): m/z $[M + H]^+$ calcd for $[C_{59}H_{48}N_5O_4]^+$ 890.3701; found 890.3710 (error = 1.0 ppm). UV/vis (CH_2Cl_2, nm): λ_{max} (ε_{max} M^{-1} cm^{-1}) = 477 (56 400), 447 (31 200), 432 (26 100), 408 (13 300), 337 (30 500).

*N,N′-Bis(2′,6′-diisopropylphenyl)-13-phenyl-azabenzo[pqr]-perylene-3,4:9,10-tetracarboxylic Acid Bisimide (**3e**).* The reaction was performed according to the general Pictet–Spengler reaction procedure using 523 mg (0.69 mmol) of amino-PBI **1** and 1.48 g (13.9 mmol) of benzaldehyde **2e**. The product was obtained as a yellow solid after column chromatography (SiO_2, 99:1 CH_2Cl_2/MeOH) and recrystallization (MeOH). The analytical data are in agreement with those described in the literature.[22] Yield: 0.21 g (0.26 mmol, 38%). Mp > 300 °C. ^{1}H NMR (400 MHz, CD_2Cl_2): δ = 9.68 (s, 1H), 9.67 (s, 1H), 9.52–9.48 (m, 2H), 9.26 (d, ^3J = 8.2 Hz, 1H), 9.23 (d, ^3J = 8.2 Hz, 1H), 8.08–8.06 (m, 2H), 7.79–7.69 (m, 3H), 7.60–7.54 (m, 2H), 7.44–7.39 (m, 4H), 2.95–2.82 (m, 4H), 1.23–1.17 (m, 24H). ^{13}C NMR (100 MHz, CD_2Cl_2): δ = 164.4, 164.20, 164.15, 164.0, 162.0, 146.54, 146.46, 145.0, 139.0, 135.9, 135.4, 133.9, 133.5, 131.7, 131.5, 131.4, 131.3, 130.3, 130.22, 130.18, 130.1, 130.0, 129.33, 129.29, 127.6, 126.4, 124.8, 124.6, 124.5, 124.4, 124.2, 124.1, 124.0, 123.6, 122.7, 122.6, 119.7, 29.7, 29.6, 24.19, 24.17, 24.16, 24.1. MS (MALDI-TOF, matrix, DCTB; mode, positive): m/z calcd for $[C_{55}H_{45}N_3O_4]^+$ 811.34; found 810.95. HRMS (ESI-TOF, positive, acetonitrile/chloroform): m/z $[M + H]^+$ calcd for $[C_{55}H_{46}N_3O_4]^+$ 812.3488; found 812.3483 (error = 0.8 ppm). UV/vis (CH_2Cl_2, nm): λ_{max} (ε_{max} M^{-1} cm^{-1}) = 477 (59 500), 447 (33 000), 428 (26 100), 405 (13 200), 327 (26 400), 296 (27 600). CV (CH_2Cl_2, 0.1 M $TBAPF_6$, V vs Fc^+/Fc): $E_{1/2}$ = −1.04 ($PBI^{-/0}$), −1.35 ($PBI^{2-/-}$).

*N,N′-Bis(2′,6′-diisopropylphenyl)-13-(3″-(pyridin-2‴-yl)-phenyl)-azabenzo[pqr]-perylene-3,4:9,10-tetracarboxylic Acid Bisimide (**3f**).* The reaction was performed according to the general Pictet–Spengler reaction procedure using 594 mg (0.82 mmol) of amino-PBI **1** and 630 mg (3.44 mmol) of 3-pyridin-2′-yl-benzaldehyde **2f**. The product was obtained as a yellow solid after column chromatography (SiO_2, 95:5 CH_2Cl_2/EtOAc) and recrystallization (2:2:1 n-hexane/EtOAc/$CHCl_3$). Yield: 155 mg (0.17 mmol, 21%). Mp > 300 °C. ^{1}H NMR (400 MHz, CD_2Cl_2): δ = 9.80 (s, 1H), 9.76 (s, 1H), 9.59–9.57 (m, 2H), 9.32 (d, ^3J = 8.3 Hz, 1H), 9.27 (d, ^3J = 8.1 Hz, 1H), 8.77 (m, 1H), 8.72 (ddd, ^3J = 4.8 Hz, ^4J = 1.8 Hz, ^5J = 0.9 Hz, 1H), 8.36 (ddd, ^3J = 7.9 Hz, ^4J = 1.8 and 1.1 Hz, 1H), 8.18 (ddd, ^3J = 7.6 Hz, ^4J = 1.8 and 1.2 Hz, 1H), 7.97 (ddd, ^3J = 8.0 Hz, ^4J = 1.2 Hz, ^5J = 0.8 Hz, 1H), 7.90 (t, ^3J = 7.6 Hz, 1H), 7.84 (td, ^3J = 7.6 Hz, ^4J = 1.8 Hz, 1H), 7.63–7.57 (m, 2H), 7.47–7.42 (m, 4H), 7.32 (ddd, ^3J = 7.5 and 4.8 Hz, ^4J = 1.1 Hz, 1H), 2.97–2.85 (m, 4H), 1.25–1.19 (m, 24H). ^{13}C NMR (100 MHz, CD_2Cl_2): δ = 164.0, 163.84, 163.79, 163.7, 161.4, 156.4, 149.8, 146.1, 146.0, 144.7, 140.2, 139.0, 136.9, 135.6, 135.1, 133.6, 133.2, 131.3, 131.2, 131.1, 131.0, 130.0, 129.9, 129.7, 129.6, 129.3, 128.9, 128.1, 127.3, 126.0, 124.5, 124.19, 124.16, 123.83, 123.76, 123.6, 123.1, 122.6, 122.3, 122.2, 120.6, 119.4, 29.24, 29.20, 23.8. MS (MALDI-TOF, matrix, DCTB; mode, negative): m/z calcd for $[C_{60}H_{48}N_4O_4]^-$ 888.37; found 888.31. HRMS (ESI-TOF, positive, acetonitrile/chloroform): m/z $[M + H]^+$ calcd for $[C_{60}H_{49}N_4O_4]^+$ 889.3748; found 889.3758 (error = 1.1 ppm). UV/vis (CH_2Cl_2, nm): λ_{max} (ε_{max} M^{-1} cm^{-1}) = 477 (60 400), 447 (33 300), 429 (27 300), 406 (13 300), 328 (29 000), 283 (36 000).

*13-(Pyridin-2″-yl)-azabenzo[pqr]-perylene-3,4,9,10-tetracarboxylic Acid Tetrabutyl Ester (ab-PTE, **5**).* The reaction was performed according to the general Pictet–Spengler reaction procedure using 1.3 g (1.95 mmol) of amino-PTE **4**[37] and 2.5 g (23.4 mmol) of pyridine-2-carboxaldehyde **2a**. The product was obtained as a bright yellow solid after column chromatography (SiO_2, 99:1 → 97:3 CH_2Cl_2/EtOAc) and recrystallization (1:1 n-hexane/CH_2Cl_2). Yield: 911 mg (1.21 mmol, 62%). Mp 128–131 °C. ^{1}H NMR (400 MHz, $CDCl_3$): δ = 9.55 (s, 1H), 9.12 (d, ^3J = 8.3 Hz, 2H), 8.99 (s, 1H), 8.88 (ddd, ^3J = 4.9 Hz, ^4J = 1.7 Hz, ^5J = 0.8 Hz, 1H), 8.58 (d, ^3J = 8.2 Hz, 1H), 8.50 (d, ^3J = 8.1 Hz, 1H), 8.33 (ddd, ^3J = 7.8 Hz, ^4J = 1.2 Hz, ^5J = 0.8 Hz, 1H), 8.00 (td, ^3J = 7.7 Hz, ^4J = 1.8 Hz, 1H), 7.49 (ddd, ^3J = 7.6 and 4.8 Hz, ^4J = 1.2 Hz, 1H), 4.41–4.30 (m, 8H), 1.83–1.68 (m, 8H), 1.54–1.39 (m, 8H), 0.98–0.90 (m, 12H). ^{13}C NMR (100 MHz, $CDCl_3$): δ = 168.7, 168.5, 168.42, 168.36, 157.7, 156.0, 149.1, 143.2, 137.4, 133.5, 133.1, 133.0, 132.0, 131.3, 130.91, 130.88, 130.1, 129.6, 129.5, 127.7, 126.13, 126.11, 125.6, 125.3, 123.8, 122.6, 122.3, 121.2, 118.8, 65.8, 65.73, 65.69, 65.5, 30.74, 30.66, 30.64, 30.61, 19.33, 19.31, 19.30, 19.28, 13.8. MS (MALDI-TOF, matrix, DCTB; mode, positive): m/z calcd for $[C_{46}H_{46}N_2O_8]^+$ 754.33; found 754.34. HRMS (ESI-TOF, positive, acetonitrile/chloroform): m/z $[M + H]^+$ calcd for $[C_{46}H_{47}N_2O_8]^+$ 755.3327; found 755.3336 (error = 1.2 ppm). UV/vis (CH_2Cl_2, nm): λ_{max} (ε_{max} M^{-1} cm^{-1}) = 430 (25 700), 407 (24 000), 394 (24 100), 319 (43 400). CV (CH_2Cl_2, 0.1 M $TBAPF_6$, V vs Fc^+/Fc): $E_{1/2}$ = −1.60 ($PBI^{-/0}$), −1.88 ($PBI^{2-/-}$).

*13-(Pyridin-2″-yl)-azabenzo[pqr]-perylene-3,4:9,10-tetracarboxylic Acid Bisanhydride (ab-PBA, **6**).* Ab-PTE **5** (679 mg, 0.899 mmol) was dissolved in 79 mL of glacial acid and 1.7 mL of concentrated sulfuric acid. The reaction mixture was heated to 130 °C, and after 5 h reaction time a suspension was obtained. Subsequently, 100 mL of water was added to the reaction mixture, and the brown precipitate was separated by filtration and washed successively with acetone, methanol, and dichloromethane. High vacuum drying at 60 °C afforded an ocher-colored solid. Yield: 368 mg (0.74 mmol, 83%). Mp > 300 °C. ^{1}H NMR (400 MHz, D_2SO_4): δ = 10.68–10.62 (m, 2H), 10.50 (s, 1H), 10.30 (d, ^3J = 8.3 Hz, 1H), 10.25 (d, ^3J = 8.2 Hz, 1H), 10.20 (s, 1H), 10.00 (bd, ^3J = 5.6 Hz, 1H), 9.88 (bt, ^3J = 8.2 Hz, 1H), 9.55 (bd, ^3J = 7.7 Hz, 1H), 9.40–9.36 (m, 1H). ^{13}C NMR (100 MHz, D_2SO_4): δ = 163.0, 162.9, 162.3, 162.0, 151.3, 146.5, 144.8, 138.7, 138.6, 138.4, 136.7, 136.3, 135.3, 135.2, 134.3, 133.0, 132.9, 132.3, 131.0, 129.8, 129.5, 128.1, 126.6, 123.9, 123.7, 122.9, 122.5, 120.4, 119.4.

*N,N′-Bis(2′,5′,8′,11′,15′,18′,21′,24′-octaoxapentacosan-13′-yl)-13-(pyridin-2″-yl)-azabenzo[pqr]-perylene-3,4:9,10-tetracarboxylic Acid Bisimide (ab-PBI^{OEG}, **8**).* The ab-PBA **6** (50 mg, 0.101 mmol), 2,5,8,11,15,18,21,24-octaoxapentacosan-13-amine (**7**, 105 mg, 0.275 mmol), imidazole (500 mg), and pyridine (50 μL) were placed in a reaction flask under inert conditions. Afterward, the reaction mixture was heated to 120 °C, and the brownish suspension turned slowly into a green solution. After 3 h, the warm reaction mixture (~50 °C) was quenched by the addition of 2 mL of 2 N hydrochloric acid and 5 mL

DOI: 10.1021/acs.joc.6b01573
J. Org. Chem. 2016, 81, 8394–8405

of dichloromethane. The organic phase was separated and washed twice with 5 mL of water. The crude product was purified by column chromatography (SiO_2, 99:1 CH_2Cl_2/methanol) to yield an orange solid. Yield: 89 mg (0.073 mmol, 72%). Mp 261−263 °C. ^{1}H NMR (400 MHz, $CDCl_3$): δ = 10.16 (bs, 1H), 9.33 (bs, 1H), 9.11−9.08 (m, 2H), 8.99−8.91 (m, 3H), 8.45 (ddd, ^3J = 7.8 Hz, ^4J = 1.2 Hz, ^5J = 0.8 Hz, 1H), 8.07 (td, ^3J = 7.7 Hz, ^4J = 1.7 Hz, 1H), 7.54 (ddd, ^3J = 7.8 and 4.8 Hz, ^4J = 1.1 Hz, 1H), 5.80−5.72 (m, 2H), 4.24−4.19 (m, 4H), 3.99−3.97 (m, 4H), 3.76−3.50 (m, 25H), 3.48−3.45 (m, 15H), 3.40−3.37 (m, 8H), 3.23 (s, 6H), 3.22 (s, 6H). ^{13}C NMR (100 MHz, $CDCl_3$): δ = 164.09, 164.05, 164.0, 163.8, 157.12, 157.08, 149.3, 143.7, 137.6, 134.0, 132.7, 129.3, 128.0, 126.6, 126.2, 124.2, 123.9, 123.5, 122.7, 122.4, 122.0, 119.0, 71.8, 70.54, 70.52, 70.49, 70.44, 70.43, 70.40, 69.4, 59.0, 52.5. MS (MALDI-TOF, matrix, DCTB; mode, negative): m/z calcd for $[C_{64}H_{80}N_4O_{20}]^-$ 1224.54; found 1224.48. HRMS (ESI-TOF, positive, methanol/chloroform): m/z $[M + H]^+$ calcd for $[C_{64}H_{81}N_4O_{20}]^+$ 1225.5439; found 1225.5450 (error = 0.9 ppm). UV/vis (CH_2Cl_2, nm): λ_{max} (ε_{max} M^{-1} cm^{-1}) = 473 (60 300), 444 (32 900), 430 (24 100), 405 (12 200), 333 (26 200), 307 (28 300).

*N-(12′-Tricosanyl)-1-nitro-perylene-3,4-dicarboxylic Acid Monoimide-9,10- dicarboxylic Acid Dioctyl Ester (1-Nitro-PMIDE, **10**).* PMIDE **9**[38] (99 mg, 104 μmol) and cerium(IV) ammonium nitrate (88 mg, 160 μmol) were dissolved in 12 mL of dry dichloromethane under inert conditions. Afterward, fuming nitric acid (0.15 mL, 3.60 mmol) was added to the orange solution, and an immediate color change to dark red occurred. The completion of the conversion was monitored by TLC (SiO_2, 1:1 CH_2Cl_2/n-hexane). After 15 min, the reaction was quenched by the addition of 2 N NaOH aqueous solution to adjust the pH to ∼7. The pH neutral reaction mixture was extracted twice with 100 mL each of dichloromethane. The crude product was purified by column chromatography (SiO_2, CH_2Cl_2/n-hexane: 1:1.2 → 1:1) to obtain a dark red solid. Yield: 90 mg (0.09 mmol, 86%). Mp < 30 °C. ^{1}H NMR (400 MHz, CD_2Cl_2): δ = 8.53 (bs, 2H), 8.35 (d, ^3J = 8.3 Hz, 1H), 8.30 (d, ^3J = 8.1 Hz, 1H), 7.97 (d, ^3J = 8.0 Hz, 1H), 7.85 (d, ^3J = 8.0 Hz, 1H), 7.80 (d, ^3J = 8.0 Hz, 1H), 5.10−5.02 (m, 1H), 4.24−4.19 (m, 4H), 2.17−2.09 (m, 2H), 1.79−1.65 (m, 6H), 1.38−1.11 (m, 56H), 0.84−0.72 (m, 12H). ^{13}C NMR (100 MHz, CD_2Cl_2): δ = 167.9, 167.7, 147.4, 133.7, 132.7, 131.1, 130.5, 130.1, 129.5, 129.3, 128.8, 128.0, 127.6, 127.3, 126.1, 123.9, 66.2, 66.1, 55.0, 32.3, 32.0, 29.8, 29.7, 29.6, 29.5, 29.4, 29.3, 28.7, 27.0, 26.1, 22.8, 14.01, 14.00. MS (MALDI-TOF, matrix, DCTB; mode, negative): m/z calcd for $[C_{63}H_{88}N_2O_8]^-$ 1000.65; found 1000.64. HRMS (ESI-TOF, positive, acetonitrile/chloroform): m/z $[M + H]^+$ calcd for $[C_{63}H_{89}N_2O_8]^+$ 1001.6619; found 1001.6613 (error = 0.6 ppm). UV/vis (CH_2Cl_2, nm): λ_{max} (ε_{max} M^{-1} cm^{-1}) = 503 (27 200), 361 (6600), 266 (21 300).

*N-(12′-Tricosanyl)-1-amino-perylene-3,4-dicarboxylic Acid Monoimide-9,10-dicarboxylic Acid Dioctyl Ester (1-Amino-PMIDE, **11**).* 1-Nitro-PMIDE **10** (90 mg, 90 μmol) and tin(II) chloride dihydrate (260 mg, 1.15 mmol) were suspended in 8 mL of tetrahydrofuran. After the reaction mixture was purged with nitrogen for 40 min, the solution was heated to reflux under inert conditions. The completion of the conversion was monitored by TLC (SiO_2, 100:1 CH_2Cl_2/MeOH). After 1 h reaction time, the solvent was removed under reduced pressure, and the violet solid was dissolved in dichloromethane. The organic solution was washed three times with 100 mL each of water and twice with 50 mL each of sodium hydrogen carbonate solution. The crude product was purified by column chromatography (SiO_2, 100:1 CH_2Cl_2/MeOH) to yield a violet solid. Yield: 31 mg (32 μmol, 36%). Mp < 30 °C. ^{1}H NMR (400 MHz, $CDCl_3$): δ = 8.61 (d, ^3J = 8.1 Hz, 1H), 8.34−8.25 (m, 1H), 8.21 (d, ^3J = 8.3 Hz, 1H), 8.14 (d, ^3J = 8.3 Hz, 1H), 8.08−8.01 (m, 1H), 7.99 (d, ^3J = 8.3 Hz, 1H), 7.96 (d, ^3J = 7,9 Hz, 1H), 7.19 (s, 2H), 5.09 (bs, 1H), 4.29−4.22 (m, 4H), 2.24−2.10 (m, 2H), 1.83−1.67 (m, 6H), 1.44−1.05 (m, 56H), 0.81 (t, ^3J = 6.1 Hz, 6H), 0.77 (t, ^3J = 6.7 Hz, 6H). ^{13}C NMR (100 MHz, $CDCl_3$): δ = 168.6, 168.5, 144.6, 133.7, 133.6, 132.9, 130.39, 130.37, 130.2, 130.0, 129.5, 129.2, 129.0, 128.8, 128.1, 123.7, 122.8, 122.4, 120.8, 65.8, 65.7, 54.6, 32.4, 31.9, 31.8, 29.64, 29.61, 29.59, 29.3, 29.2, 28.6, 27.0, 26.1, 22.7, 14.13, 14.12. MS (MALDI-TOF, matrix, DCTB; mode, negative): m/z calcd for $[C_{63}H_{90}N_2O_6]^-$ 970.68; found 970.68. HRMS (ESI-TOF, positive, acetonitrile/chloroform): m/z $[M + H]^+$ calcd for $[C_{63}H_{91}N_2O_6]^+$ 971.6877; found 971.6872 (error = 0.5 ppm). UV/vis (CH_2Cl_2, nm): λ_{max} (ε_{max} M^{-1} cm^{-1}) = 535 (8200), 410 (3300), 276 (9300).

*N-(12′-Tricosanyl)-13-(pyridin-2″-yl)-azabenzo[pqr]-perylene-3,4-dicarboxylic Acid Monoimide-9,10-dicarboxylic Acid Dioctyl Ester (ab-PMIDE, **12**).* The reaction was performed according to the general Pictet−Spengler reaction procedure using 580 mg (0.60 mmol) of 1-amino-PMIDE **11** and 0.77 g (7.23 mmol) of pyridine-2-carboxaldehyde **2a**. The product was obtained as a yellow-orange solid after column chromatography (SiO_2, gradual CH_2Cl_2 → 9:1 CH_2Cl_2/MeOH). Yield: 388 mg (0.37 mmol, 61%). Mp < 30 °C. ^{1}H NMR (400 MHz, CD_2Cl_2): δ = 9.52 (s, 1H), 8.91−8.84 (m, 1H), 8.82 (ddd, ^3J = 4.8 Hz, ^4J = 1.8 Hz, ^5J = 0.9 Hz, 1H), 8.49 (ddd, ^3J = 7.8 Hz, ^4J = 1.2 Hz, ^5J = 0.8 Hz, 1H), 8.47−8.39 (m, 1H), 8.39−8.29 (m, 2H), 8.21−8.13 (m, 1H), 8.06 (td, ^3J = 7.8 Hz, ^4J = 1.8 Hz, 1H), 7.50 (ddd, ^3J = 7.8 Hz, 4.8 Hz, ^4J = 1.2 Hz, 1H), 5.17 (bs, 1H), 4.39−4.28 (m, 4H), 2.25 (bs, 2H), 1.93 (bs, 2H), 1.88−1.76 (m, 4H), 1.53−1.42 (m, 4H), 1.42−1.02 (m, 52H), 0.86−0.77 (m, 6H), 0.76 (t, ^3J = 6.7 Hz, 6H). ^{13}C NMR (100 MHz, CD_2Cl_2): δ = 168.1, 167.9, 164.6, 164.3, 163.6, 163.1, 157.5, 155.2, 148.6, 142.5, 137.2, 134.3, 133.6, 132.1, 131.1, 130.4, 129.1, 128.4, 127.4, 127.1, 126.4, 125.7, 125.2, 124.6, 123.8, 122.3, 122.1, 122.0, 121.5, 121.2, 121.1, 118.3, 66.1, 65.9, 54.7, 32.6, 32.4, 31.9, 29.7, 29.6, 29.5, 29.4, 29.3, 29.2, 28.8, 28.7, 27.2, 26.2, 26.1, 22.7, 22.6, 13.9, 13.8. MS (MALDI-TOF, matrix, DCTB; mode, positive): m/z calcd for $[C_{69}H_{91}N_3O_6]^+$ 1057.69; found 1057.67. HRMS (ESI-TOF, positive, acetonitrile/chloroform): m/z $[M + H]^+$ calcd for $[C_{69}H_{92}N_3O_6]^+$ 1058.6981; found 1058.6979 (error = 0.2 ppm). UV/vis (CH_2Cl_2, nm): λ_{max} (ε_{max} M^{-1} cm^{-1}) = 454 (36 900), 427 (22 900), 413 (22 600), 392 (11 800), 317 (29 800). CV (CH_2Cl_2, 0.1 M $TBAPF_6$, V vs Fc^+/Fc): $E_{1/2}$ = −1.35 ($PBI^{-/0}$), −1.64 ($PBI^{2-/-}$).

*N-(12′-Tricosanyl)-13-(pyridin-2″-yl)-azabenzo[pqr]-perylene-3,4-dicarboxylic Acid Monoimide-9,10-dicarboxylic Acid Monoanhydride (ab-PMIMA, **13**).* The ab-PMIDE **12** (298 mg, 282 μmol) was dissolved in 25 mL of glacial acid and 0.6 mL of concentrated sulfuric acid and heated to 130 °C. After 5 h of reaction time, an orange suspension was formed, and the completion of the reaction was monitored by TLC (SiO_2, 99:1 CH_2Cl_2/MeOH). Subsequently, 200 mL of water was added to the reaction mixture. The orange precipitate was separated by filtration and washed pH neutral with water. The solid was redissolved in a 9:1 dichloromethane/methanol mixture and directly used for size exclusion chromatography (Bio-Beads S-X3, 9:1 CH_2Cl_2/MeOH) to isolate the product as an orange solid. Yield: 157 mg (0.19 mmol, 68%). Mp < 30 °C. ^{1}H NMR (400 MHz, CD_2Cl_2): δ = 9.62 (s, 1H), 8.76−8.74 (m, 2H), 8.59 (bs, 1H), 8.42 (d, ^3J = 8.3 Hz, 1H), 8.27−8.21 (m, 2H), 8.18 (ddd, ^3J = 7.8 Hz, ^4J = 1.2 Hz, ^5J = 0.7 Hz, 1H), 7.96 (td, ^3J = 7.7 Hz, ^4J = 1.8 Hz, 1H), 7.50 (ddd, ^3J = 7.6 and 4.8 Hz, ^4J = 1.1 Hz, 1H), 5.22−5.14 (m, 1H), 2.28−2.26 (m, 2H), 2.00−1.95 (m, 2H), 1.41−1.14 (m, 36H), 0.74 (t, ^3J = 6.9 Hz, 6H). ^{13}C NMR (100 MHz, CD_2Cl_2): δ = 163.7, 162.7, 159.0, 158.9, 156.0, 154.9, 148.9, 143.2, 137.6, 135.6, 133.8, 133.6, 133.1, 131.1, 130.2, 129.4, 128.8, 128.2, 127.8, 126.7, 126.0, 125.4, 124.6, 124.0, 123.7, 123.3, 122.6, 121.4, 120.6, 119.9, 118.1, 116.74, 116.70, 55.2, 32.4, 31.9, 29.8, 29.73, 29.70, 29.4, 27.2, 22.7, 13.9. MS (MALDI-TOF, matrix, DCTB; mode, negative): m/z calcd for $[C_{53}H_{57}N_3O_5]^+$ 815.43; found 815.38. HRMS (ESI-TOF, positive, acetonitrile/chloroform): m/z $[M + H]^+$ calcd for $[C_{53}H_{58}N_3O_5]^+$ 816.4371; found 816.4336 (error = 4.2 ppm). UV/vis (CH_2Cl_2, nm): λ_{max} (ε_{max} M^{-1} cm^{-1}) = 469 (41 700), 472 (24 500), 323 (25 800). CV (CH_2Cl_2, 0.1 M $TBAPF_6$, V vs Fc^+/Fc): $E_{1/2}$ = −1.05 ($PBI^{-/0}$), −1.31 ($PBI^{2-/-}$).

*N,N′-Bis(2′,6′-diisopropylphenyl)-anti-13,14-di((pyridin-2″-yl)-azabenzo[pqr])-perylene-3,4:9,10-tetracarboxylic Acid Bisimide (anti-(ab)$_2$-PBI, **15**) and N,N′-Bis(2′,6′-diisopropylphenyl)-syn-13,14-di((pyridin-2″-yl)-azabenzo[pqr])-perylene-3,4:9,10-tetracarboxylic Acid Bisimide (syn-(ab)$_2$-PBI, **16**).* The reaction was performed according to the general Pictet−Spengler reaction procedure using 1.36 g (1.84 mmol) of a 1,7- and 1,6-diamino-PBI isomer mixture **14** (3:2) and 1.86 g (17.3 mmol) of pyridine-2-carboxaldehyde **2a**. The crude product was first purified by column

DOI: 10.1021/acs.joc.6b01573
J. Org. Chem. 2016, 81, 8394−8405

chromatography (SiO_2, CH_2Cl_2/MeOH, 99:1) to obtain 638 mg (0.697 mmol, 38%) of the isomeric mixture (*anti*-(ab)$_2$-PBI) and *syn*-(ab)$_2$-PBI). After multiple column chromatography (SiO_2, dry packed, 3:1:3 CH_2Cl_2/EtOAc/*n*-hexane), 382 mg (0.417 mmol, 23%) of the orange *anti*-(ab)$_2$-PBI **15** and 236 mg (0.258 mmol, 14%) of the yellow *syn*-(ab)$_2$-PBI **16** were isolated (isomer ratio ∼3:2). The analytical data of *syn*-(ab)$_2$-PBI match those reported in the literature.[22] Single crystals suitable for X-ray diffraction were grown by slow evaporation of a saturated solution of *anti*-(ab)$_2$-PBI **15** in THF at room temperature. *anti*-(ab)$_2$-PBI **15**: Mp > 300 °C. ^{1}H NMR (400 MHz, d_8-THF, 233 K): δ = 10.57 (s, 2H), 9.78 (s, 2H), 8.99 (d, ^3J = 7.6 Hz, 2H), 8.43 (d, ^3J = 4.4 Hz, 2H), 8.40 (td, ^3J = 7.4 Hz, ^4J = 1.0 Hz, 2H), 7.77 (ddd, ^3J = 7.5 and 4.8 Hz, ^4J = 0.8 Hz, 2H), 7.72 (dd, ^3J = 8.2 Hz, ^4J = 1.0 Hz, 2H), 7.64 (t, ^3J = 8.2 Hz, 2H), 7.44 (dd, ^3J = 7.9 Hz, ^4J = 1.0 Hz, 2H), 4.20 (sep, ^3J = 6.2 Hz, 2H), 2.66 (sep, ^3J = 6.6 Hz, 2H), 2.00−1.94 (m, 12H), 1.04 (d, ^3J = 6.7 Hz, 6H), 0.99 (d, ^3J = 6.7 Hz, 6H). ^{13}C NMR (100 MHz, d_8-THF, 233 K): δ = 164.2, 163.9, 158.4, 158.3, 149.3, 147.8, 146.2, 142.0, 138.7, 133.7, 133.2, 132.2, 130.2, 128.2, 126.2, 125.5, 125.2, 125.1, 124.7, 124.6, 123.3, 122.4, 118.2, 117.3, 30.6, 29.9, 26.2, 25.7, 24.5, 24.0. MS (MALDI-TOF, matrix, DCTB; mode, negative): m/z calcd for $[C_{60}H_{46}N_6O_4]^-$ 914.36; found 914.31. HRMS (ESI-TOF, positive, acetonitrile/chloroform 1:1): m/z [M + H]$^+$ calcd for $[C_{60}H_{47}N_6O_4]^+$ 915.3653; found 915.3650 (error = 0.3 ppm). UV/vis (CH_2Cl_2, nm): λ_{max} (ε_{max} M^{-1} cm^{-1}) = 485 (20 500), 455 (11 000), 414 (46 600), 393 (25 800), 355 (85 400), 338 (64 100). CV (CH_2Cl_2, 0.1 M $TBAPF_6$, V vs Fc^+/Fc): $E_{1/2}$ = +1.91 (PBI$^{+/0}$, irrev), −1.13 (PBI$^{-/0}$), −1.43 (PBI$^{2-/-}$). *syn*-(ab)$_2$-PBI **16**: Mp > 300 °C. ^{1}H NMR (400 MHz, $CDCl_3$): δ = 11.13 (s, 2H), 10.29 (s, 2H), 9.01 (ddd, ^3J = 4.8 Hz, ^4J = 1.7 Hz, ^5J = 0.9 Hz, 2H), 8.73 (ddd, ^3J = 7.8 Hz, ^4J = 1.2 Hz, ^5J = 0.8 Hz, 2H), 8.15 (td, ^3J = 7.7 Hz, ^4J = 1.8 Hz, 2H), 7.61 (ddd, ^3J = 7.7 and 4.8 Hz, ^4J = 1.1 Hz, 2H), 7.54−7.47 (m, 2H), 7.40−7.34 (m, 4H), 2.95 (sep, ^3J = 6.7 Hz, 2H), 2.86 (sep, ^3J = 6.9 Hz, 2H), 1.20 (d, ^3J = 6.9 Hz, 12H), 1.16 (d, ^3J = 6.9 Hz, 12H). ^{13}C NMR (100 MHz, $CDCl_3$): δ = 164.2, 164.1, 158.9, 157.5, 149.4, 145.80, 145.76, 143.5, 138.0, 134.8, 132.8, 130.74, 130.68, 130.0, 129.8, 128.8, 127.7, 126.4, 125.4, 124.7, 124.4, 124.2, 123.7, 123.0, 122.5, 120.6, 119.6, 118.6, 29.5, 29.4, 24.2, 24.1. MS (MALDI-TOF, matrix, DCTB; mode, negative): m/z calcd for $[C_{60}H_{46}N_6O_4]^-$ 914.36; found 914.32. HRMS (ESI-TOF, positive, acetonitrile/chloroform 1:1): m/z [M + H]$^+$ calcd for $[C_{60}H_{47}N_6O_4]^+$ 915.3653; found 915.3656 (error = 0.3 ppm). UV/vis (CH_2Cl_2, nm): λ_{max} (ε_{max} M^{-1} cm^{-1}) = 478 (4800), 448 (6800), 429 (42 100), 405 (25 600), 356 (82 900). CV (CH_2Cl_2, 0.1 M $TBAPF_6$, V vs Fc^+/Fc): $E_{1/2}$ = +1.87 (PBI$^{+/0}$, irrev), −1.16 (PBI$^{-/0}$), −1.44 (PBI$^{2-/-}$).

syn-13,14-Di((pyridin-2″-yl)-azabenzo[pqr])-perylene-3,4,9,10-tetracarboxylic Acid Tetrabutyl Ester (syn-(ab)$_2$-PTE, ***18****).* The reaction was performed according to the general Pictet−Spengler reaction procedure using 0.29 g (0.43 mmol) of 1,6-diamino-PTE **17** and 0.91 g (8.5 mmol) of pyridine-2-carboxaldehyde **2a**. The product was obtained as a bright-yellow solid after column chromatography (SiO_2, 99:1 CH_2Cl_2/MeOH) and recrystallization (*n*-hexane/CH_2Cl_2). Yield: 135 mg (0.16 mmol, 37%). Mp 207−208 °C. ^{1}H NMR (400 MHz, $CDCl_3$): δ = 10.37 (s, 2H), 9.62 (s, 2H), 8.98 (ddd, ^3J = 4.8 Hz, ^4J = 1.7 Hz, ^5J = 0.9 Hz, 2H), 8.56 (ddd, ^3J = 7.8 Hz, ^4J = 1.2 Hz, ^5J = 0.8 Hz, 2H), 8.10 (td, ^3J = 7.8 Hz, ^4J = 1.7 Hz, 2H), 7.57 (ddd, ^3J = 7.7 and 4.8 Hz, ^4J = 1.1 Hz, 1H), 4.53 (t, ^3J = 6.8 Hz, 4H), 4.44 (t, ^3J = 6.7 Hz, 4H), 1.92−1.85 (m, 4H), 1.81−1.74 (m, 4H), 1.61−1.53 (m, 4H), 1.50−1.43 (m, 4H), 0.99 (t, ^3J = 7.3 Hz, 6H), 0.94 (t, ^3J = 7.4 Hz, 6H). ^{13}C NMR (100 MHz, $CDCl_3$): δ = 168.7, 168.5, 157.9, 157.6, 149.3, 142.4, 137.6, 132.9, 132.4, 131.6, 130.5, 128.1, 127.0, 126.3, 124.1, 122.8, 122.5, 121.8, 121.1, 117.7, 66.1, 65.9, 30.8, 30.6, 19.4, 19.3, 13.9, 13.9. MS (MALDI-TOF, matrix, DCTB; mode, positive): m/z calcd for $[C_{52}H_{48}N_4O_8 + H]^+$ 857.35; found 857.25. HRMS (ESI-TOF, positive, methanol/chloroform 1:1): m/z [M + H]$^+$ calcd for $[C_{52}H_{49}N_4O_8]^+$ 857.3545; found 857.3551 (error = 0.7 ppm). UV/vis (CH_2Cl_2, nm): λ_{max} (ε_{max} M^{-1} cm^{-1}) = 445 (1800), 420 (2400), 384 (18 400), 370 (28 300), 336 (118 800). CV (CH_2Cl_2, 0.1 M $TBAPF_6$, V vs Fc^+/Fc): $E_{1/2}$ = −1.68 (PBI$^{-/0}$), −1.98 (PBI$^{2-/-}$).

syn-13,14-Di((pyridin-2″-yl)-azabenzo[pqr])-perylene-3,4:9,10-tetracarboxylic Acid Bisanhydride (syn-(ab)$_2$-PBA, ***19****).* *syn*-(ab)$_2$-PTE **18** (95 mg, 0.111 mmol) was dissolved in 10 mL of glacial acid and 0.2 mL of concentrated sulfuric acid. The reaction mixture was heated to 130 °C, and after 17 h reaction time a suspension was formed. Subsequently, 200 mL of water was added to the cooled reaction mixture, and the brown precipitate was separated by filtration and washed successively with water, acetone, methanol, and dichloromethane. High vacuum drying at 60 °C afforded the product as an ocher-colored solid. Yield: 64 mg (0.11 mmol, 97%). Mp > 300 °C. ^{1}H NMR (400 MHz, D_2SO_4): δ = 11.51 (s, 2H), 11.41 (s, 2H), 10.28 (bd, ^3J = 5.8 Hz, 2H), 10.14 (bt, ^3J = 8.1 Hz, 2H), 9.91 (bd, ^3J = 7.7 Hz, 2H), 9.40−9.36 (m, 2H). ^{13}C NMR (100 MHz, D_2SO_4): δ = 160.3, 160.2, 151.7, 150.8, 147.3, 140.0, 138.0, 136.2, 135.4, 133.9, 133.8, 133.7, 132.1, 129.6, 128.5, 127.1, 124.3, 121.3, 119.1, 119.0.

■ ASSOCIATED CONTENT

Supporting Information

The Supporting Information is available free of charge on the ACS Publications website at DOI: 10.1021/acs.joc.6b01573.

Figures S1−S7, Tables S1 and S2 mentioned in the text, ^{1}H, ^{13}C NMR, MALDI, and HR-ESI-TOF mass spectra of all compounds (Figures S6−S69), as well as computational data (Cartesian coordinates, total energies, and frontier molecular orbital plots) (PDF)

X-ray data for compound **15** (CIF)

■ AUTHOR INFORMATION

Corresponding Author

*E-mail: wuerthner@chemie.uni-wuerzburg.de.

Notes

The authors declare no competing financial interest.

■ ACKNOWLEDGMENTS

This work was supported by the Bavarian Research Program “Solar Technologies Go Hybrid”. M.S. thanks the Fonds der Chemischen Industrie for a Kekulé fellowship. We thank David Bialas for his support in theoretical calculations.

■ REFERENCES

(1) Zollinger, H. *Color Chemistry: Syntheses, Properties, and Applications of Organic Dyes and Pigments*; Wiley: New York, 2003.

(2) Herbst, W.; Hunger, K. *Industrial Organic Pigments: Production, Properties, Applications*; Wiley: New York, 2006.

(3) Markiewicz, J. T.; Wudl, F. *ACS Appl. Mater. Interfaces* **2015**, *7*, 28063−28085.

(4) Weil, T.; Vosch, T.; Hofkens, J.; Peneva, K.; Müllen, K. *Angew. Chem., Int. Ed.* **2010**, *49*, 9068−9093.

(5) Adachi, M.; Nagao, Y. *Chem. Mater.* **2001**, *13*, 662−669.

(6) Sadrai, M.; Hadel, L.; Sauers, R. R.; Husain, S.; Krogh-Jespersen, K.; Westbrook, J. D.; Bird, G. R. *J. Phys. Chem.* **1992**, *96*, 7988−7996.

(7) Würthner, F.; Stolte, M. *Chem. Commun.* **2011**, *47*, 5109−5115.

(8) Li, C.; Wonneberger, H. *Adv. Mater.* **2012**, *24*, 613−636.

(9) Huang, C.; Barlow, S.; Marder, S. R. *J. Org. Chem.* **2011**, *76*, 2386−2407.

(10) Lee, S. K.; Zu, Y.; Herrmann, A.; Geerts, Y.; Müllen, K.; Bard, A. J. *J. Am. Chem. Soc.* **1999**, *121*, 3513−3520.

(11) Chen, L.; Li, C.; Müllen, K. *J. Mater. Chem. C* **2014**, *2*, 1938−1956.

(12) Battagliarin, G.; Li, C.; Enkelmann, V.; Müllen, K. *Org. Lett.* **2011**, *13*, 3012−3015.

(13) Nakazono, S.; Easwaramoorthi, S.; Kim, D.; Shinokubo, H.; Osuka, A. *Org. Lett.* **2009**, *11*, 5426−5429.

(14) Nakazono, S.; Imazaki, Y.; Yoo, H.; Yang, J.; Sasamori, T.; Tokitoh, N.; Cédric, T.; Kageyama, H.; Kim, D.; Shinokubo, H.; Osuka, A. *Chem. - Eur. J.* **2009**, *15*, 7530−7533.

DOI: 10.1021/acs.joc.6b01573
J. Org. Chem. 2016, 81, 8394−8405

(15) Teraoka, T.; Hiroto, S.; Shinokubo, H. *Org. Lett.* **2011**, *13*, 2532–2535.
(16) Battagliarin, G.; Zhao, Y.; Li, C.; Müllen, K. *Org. Lett.* **2011**, *13*, 3399–3401.
(17) Ito, S.; Hiroto, S.; Shinokubo, H. *Org. Lett.* **2013**, *15*, 3110–3113.
(18) Osswald, P.; Würthner, F. *J. Am. Chem. Soc.* **2007**, *129*, 14319–14326.
(19) Langhals, H.; Kirner, S. *Eur. J. Org. Chem.* **2000**, *2000*, 365–380.
(20) Rajasingh, P.; Cohen, R.; Shirman, E.; Shimon, L. J. W.; Rybtchinski, B. *J. Org. Chem.* **2007**, *72*, 5973–5979.
(21) Lütke Eversloh, C.; Li, C.; Müllen, K. *Org. Lett.* **2011**, *13*, 4148–4150.
(22) Hao, L.; Jiang, W.; Wang, Z. *Tetrahedron* **2012**, *68*, 9234–9239.
(23) Müller, S.; Müllen, K. *Chem. Commun.* **2005**, 4045–4046.
(24) Golubkov, G.; Weissman, H.; Shirman, E.; Wolf, S. G.; Pinkas, I.; Rybtchinski, B. *Angew. Chem., Int. Ed.* **2009**, *48*, 926–930.
(25) Kossoy, E.; Weissman, H.; Rybtchinski, B. *Chem. - Eur. J.* **2015**, *21*, 166–176.
(26) Gunderson, V. L.; Krieg, E.; Vagnini, M. T.; Iron, M. A.; Rybtchinski, B.; Wasielewski, M. R. *J. Phys. Chem. B* **2011**, *115*, 7533–7540.
(27) Rachford, A. A.; Goeb, S.; Castellano, F. N. *J. Am. Chem. Soc.* **2008**, *130*, 2766–2767.
(28) Prusakova, V.; McCusker, C. E.; Castellano, F. N. *Inorg. Chem.* **2012**, *51*, 8589–8598.
(29) Schulze, M.; Steffen, A.; Würthner, F. *Angew. Chem., Int. Ed.* **2015**, *54*, 1570–1573.
(30) Pictet, A.; Spengler, T. *Ber. Dtsch. Chem. Ges.* **1911**, *44*, 2030–2036.
(31) Cox, E. D.; Cook, J. M. *Chem. Rev.* **1995**, *95*, 1797–1842.
(32) Tsai, H.-Y.; Chen, K.-Y. *J. Lumin.* **2014**, *149*, 103–111.
(33) Tsai, H.-Y.; Chang, C.-W.; Chen, K.-Y. *Tetrahedron Lett.* **2014**, *55*, 884–888.
(34) Tsai, H.-Y.; Chen, K.-Y. *Dyes Pigm.* **2013**, *96*, 319–327.
(35) Sengupta, S.; Dubey, R. K.; Hoek, R. W. M.; van Eeden, S. P. P.; Gunbaş, D. D.; Grozema, F. C.; Sudhölter, E. J. R.; Jager, W. F. *J. Org. Chem.* **2014**, *79*, 6655–6662.
(36) Dubey, R. K.; Westerveld, N.; Grozema, F. C.; Sudhölter, E. J. R.; Jager, W. F. *Org. Lett.* **2015**, *17*, 1882–1885.
(37) Zhang, Y.; Zhao, Z.; Huang, X.; Xie, Y.; Liu, C.; Li, J.; Guan, X.; Zhang, K.; Cheng, C.; Xiao, Y. *RSC Adv.* **2012**, *2*, 12644–12647.
(38) Kelber, J.; Bock, H.; Thiebaut, O.; Grelet, E.; Langhals, H. *Eur. J. Org. Chem.* **2011**, *2011*, 707–712.
(39) Yang, X.; Xi, C.; Jiang, Y. *Tetrahedron Lett.* **2005**, *46*, 8781–8783.
(40) Amos, D. W.; Baines, D. A.; Flewett, G. W. *Tetrahedron Lett.* **1973**, *14*, 3191–3194.
(41) Fimmel, B.; Son, M.; Sung, Y. M.; Grüne, M.; Engels, B.; Kim, D.; Würthner, F. *Chem. - Eur. J.* **2015**, *21*, 615–630.
(42) Lindquist, R. J.; Phelan, B. T.; Reynal, A.; Margulies, E. A.; Shoer, L. E.; Durrant, J. R.; Wasielewski, M. R. *J. Mater. Chem. A* **2016**, *4*, 2880–2893.
(43) Marcon, R. O.; dos Santos, J. G.; Figueiredo, K. M.; Brochsztain, S. *Langmuir* **2006**, *22*, 1680–1687.
(44) Marcon, R. O.; Brochsztain, S. *Langmuir* **2007**, *23*, 11972–11976.
(45) Castellano, F. N. *Dalton Trans.* **2012**, *41*, 8493–8501.
(46) Goretzki, G.; Davies, E. S.; Argent, S. P.; Warren, J. E.; Blake, A. J.; Champness, N. R. *Inorg. Chem.* **2009**, *48*, 10264–10274.
(47) Llewellyn, B. A.; Slater, A. G.; Goretzki, G.; Easun, T. L.; Sun, X.-Z.; Davies, E. S.; Argent, S. P.; Lewis, W.; Beeby, A.; George, M. W.; Champness, N. R. *Dalton Trans.* **2014**, *43*, 85–94.
(48) Lin, M.-J.; Schulze, M.; Radacki, K.; Würthner, F. *Chem. Commun.* **2013**, *49*, 9107–9109.
(49) Merritt, L. L.; Schroeder, E. *Acta Crystallogr.* **1956**, *9*, 801–804.
(50) Nijegorodov, N.; Mabbs, R.; Downey, W. S. *Spectrochim. Acta, Part A* **2001**, *57*, 2673–2685.
(51) Avlasevich, Y.; Li, C.; Müllen, K. *J. Mater. Chem.* **2010**, *20*, 3814–3826.
(52) Ham, N. S.; Ruedenberg, K. *J. Chem. Phys.* **1956**, *25*, 13–26.
(53) Faler, C. A. *Tetrahedron Lett.* **2010**, *51*, 5621–5623.
(54) Mundinger, S.; Jakob, U.; Bichovski, P.; Bannwarth, W. *J. Org. Chem.* **2012**, *77*, 8968–8979.
(55) Samudrala, R.; Zhang, X.; Wadkins, R. M.; Mattern, D. L. *Bioorg. Med. Chem.* **2007**, *15*, 186–193.
(56) Hansen, M. R.; Schnitzler, T.; Pisula, W.; Graf, R.; Müllen, K.; Spiess, H. W. *Angew. Chem., Int. Ed.* **2009**, *48*, 4621–4624.
(57) Frisch, M. J.; Trucks, G. W.; Schlegel, H. B.; Scuseria, G. E.; Robb, M. A.; Cheeseman, J. R.; Scalmani, G.; Barone, V.; Mennucci, B.; Petersson, G. A.; Nakatsuji, H.; Caricato, M.; Li, X.; Hratchian, H. P.; Izmaylov, A. F.; Bloino, J.; Zheng, G.; Sonnenberg, J. L.; Hada, M.; Ehara, M.; Toyota, K.; Fukuda, R.; Hasegawa, J.; Ishida, M.; Nakajima, T.; Honda, Y.; Kitao, O.; Nakai, H.; Vreven, T.; Montgomery, J. A., Jr.; Peralta, J. E.; Ogliaro, F.; Bearpark, M. J.; Heyd, J.; Brothers, E. N.; Kudin, K. N.; Staroverov, V. N.; Kobayashi, R.; Normand, J.; Raghavachari, K.; Rendell, A. P.; Burant, J. C.; Iyengar, S. S.; Tomasi, J.; Cossi, M.; Rega, N.; Millam, N. J.; Klene, M.; Knox, J. E.; Cross, J. B.; Bakken, V.; Adamo, C.; Jaramillo, J.; Gomperts, R.; Stratmann, R. E.; Yazyev, O.; Austin, A. J.; Cammi, R.; Pomelli, C.; Ochterski, J. W.; Martin, R. L.; Morokuma, K.; Zakrzewski, V. G.; Voth, G. A.; Salvador, P.; Dannenberg, J. J.; Dapprich, S.; Daniels, A. D.; Farkas, Ö.; Foresman, J. B.; Ortiz, J. V.; Cioslowski, J.; Fox, D. J. *Gaussian 09*; Gaussian, Inc.: Wallingford, CT, 2009.
(58) Perdew, J. P. *Phys. Rev. B: Condens. Matter Mater. Phys.* **1986**, *33*, 8822–8824.
(59) Becke, A. D. *Phys. Rev. A: At., Mol., Opt. Phys.* **1988**, *38*, 3098–3100.
(60) Lee, C.; Yang, W.; Parr, R. G. *Phys. Rev. B: Condens. Matter Mater. Phys.* **1988**, *37*, 785–789.
(61) Weigend, F.; Ahlrichs, R. *Phys. Chem. Chem. Phys.* **2005**, *7*, 3297–3305.
(62) Sheldrick, G. *Acta Crystallogr., Sect. A: Found. Crystallogr.* **2008**, *64*, 112–122.
(63) Spek, A. *Acta Crystallogr., Sect. A* **1990**, *46*, c34.

DOI: 10.1021/acs.joc.6b01573
J. Org. Chem. 2016, 81, 8394–8405